

1
2
3
4
5
6
7
8
9
10
11
12
13
14
15
16
17
18
19
20
21
22
23
24
25
26
27
28
29

Large-scale seroepidemiology uncovers nephrological pathologies in people with tau autoimmunity

Authors:

Andreia D. Magalhães^{1†}, Marc Emmenegger^{1&}, Elena De Cecco¹, Manfredi Carta^{1‡}, Karl Frontzek^{1§}, Andra Chincisan^{1||}, Jingjing Guo¹, Simone Hornemann^{1*}, Adriano Aguzzi^{1*}

Affiliations:

¹ Institute of Neuropathology, University of Zurich; CH-8091 Zurich, Switzerland

* Correspondence: simone.hornemann@usz.ch and adriano.aguzzi@usz.ch

† Present address: Department of Neurology, Inselspital, Bern University Hospital; CH-3010 Bern, Switzerland

& Present address: Division of Medical Immunology, Department of Laboratory Medicine, University Hospital Basel; CH-4031 Basel, Switzerland

‡ Present address: Institute of Neurology, University of Zurich; CH-8091 Zurich, Switzerland

§ Present address: University College London, Institute of Neurology, Queen Square Brain Bank; WC1N 1PJ London, United Kingdom

|| Present address: Credit Suisse; CH-8001 Zurich, Switzerland

One Sentence Summary:

Anti-tau autoantibodies are prevalent, increase with age, and are associated with kidney and urinary disorders.

30 **Abstract:**

31 Intraneuronal aggregates of the microtubule-associated protein tau play a pivotal role in Alz-
32 heimer's disease and several other neurodegenerative syndromes. Anti-tau antibodies can reduce
33 pathology in mouse models of neurodegeneration and are currently being tested in humans. Here,
34 we performed a large-scale seroepidemiological search for anti-tau IgG autoantibodies ($\alpha\tau$) on
35 40,497 human plasma samples. High-titer $\alpha\tau^+$ individuals were surprisingly prevalent, with hospi-
36 tal patients being three times more likely to be $\alpha\tau^+$ ($EC_{50} \geq 2^6$) than healthy blood donors (4.8% vs
37 1.6%). Their autoantibodies bound selectively to tau, inhibited tau aggregation *in vitro*, and inter-
38 ferred with tau detection in plasma samples. No association was found between $\alpha\tau$ autoantibodies
39 and neurological disorders. Instead, tau autoreactivity showed a significant association with kidney
40 and urinary disorders (adjusted RR 1.27, 95% CI 1.10-1.45, P=0.001 and 1.40, 95% CI 1.20-1.63,
41 P<0.001 respectively). These results identify a previously unrecognized association between $\alpha\tau$
42 autoimmunity and extraneural diseases, inform clinical trials of anti-tau immunotherapies about
43 potential untoward effects, and uncover a prevalent confounder of immunoassay tau measurements
44 in plasma.

45 **Main Text:**

46 **INTRODUCTION**

47 Tau is a microtubule binding protein expressed in neurons and involved in cytoskeletal dynamics
48 (1, 2). It plays a pivotal role in a variety of neurodegenerative diseases, including Alzheimer's
49 disease (AD) (3), progressive supranuclear palsy, and various syndromes collectively referred to
50 as tauopathies (4). The presence of brain neurofibrillary tau tangles correlates with cognitive de-
51 cline (5), and plasma measurements of total and phosphorylated tau have emerged as promising
52 biomarkers for the detection and monitoring of AD progression (6-9). Moreover, active and pas-
53 sive immunization with antibodies against a wide range of tau epitopes can reduce pathology and
54 functional decline in animal models of tauopathies (10, 11) and are being tested in clinical trials
55 of neurodegenerative diseases (12).

56 Natural autoantibodies are immunoglobulins generated against self-antigens in the absence of ex-
57 ternal antigen stimulation (13). They are a normal part of the immunoglobulin repertoire and have
58 physiological roles in homeostasis and surveillance, including the clearance of cellular debris, anti-
59 inflammatory activity, and first-line defense against pathogens (14). However, in certain situations,
60 natural autoantibodies can also cause pathological autoimmunity. The study of natural autoanti-
61 bodies can therefore inform about properties of their targets, e.g. unrecognized protective or con-
62 tributing roles in disease (15). Some natural autoantibodies can cause neurological disorders, such
63 as antibodies targeting the N-methyl-D-aspartate receptor (NMDAR) in encephalitis (16) or anti-
64 bodies targeting aquaporin-4 (AQP4) in neuromyelitis optica (17). Conversely, natural antibodies
65 against amyloid- β have been suggested to protect and slow the progression of AD; aducanumab,
66 a monoclonal antibody developed from B-cells of cognitively normal older age individuals, has
67 been studied as a treatment for AD (18).

68 Anti-tau autoantibodies have been detected in plasma of patients with AD (19) and Parkinson's
69 disease (20), but also in non-neurodegeneration controls. The effects, if any, of natural anti-tau
70 autoantibodies in modulating the risk of developing neurodegenerative diseases are unknown. The
71 study of individuals with anti-tau autoantibodies could clarify their potential as modifiers or bi-
72 omarkers of disease. Here, we tested 40,497 plasma samples from healthy blood donors and from
73 patients admitted to a university hospital in the frame of a two-sites cross-sectional study. We
74 found that anti-tau autoimmunity is highly specific and surprisingly frequent, with its prevalence

75 increasing with age. Unexpectedly, natural anti-tau autoantibodies were associated with a previ-
76 ously unrecognized syndrome comprising kidney and urinary disorders.

77 RESULTS

78 Prevalence of naturally occurring plasma anti-tau autoantibodies

79 We used a cross-sectional study design to assess naturally occurring IgG autoantibodies against
80 the microtubule-binding domain of the tau protein (MTBD-tau). Plasma samples from 32,291 pa-
81 tients (age ≥ 18 years) from an unselected university hospital cohort and from 8,206 healthy blood
82 donors were screened for anti-MTBD-tau plasma IgG autoantibodies with a miniaturized ELISA
83 (Enzyme-Linked Immunosorbent Assay) in 1,536-well microplates using acoustic dispensing (21-
84 23). Each plasma sample was tested at eight serial two-fold dilutions (1:50 to 1:6,000). Optical-
85 density readings were fitted by logistic regression from which the inflexion points were derived.
86 Antibody titers were defined as “ $-\log_{10}(\text{EC}_{50})$ ”, i.e. the negative decadic logarithm of the plasma
87 dilution factor corresponding to the inflexion point of the respective regression curve.

88 After exclusion of non-informative samples (fitting error $>20\%$ $-\log_{10}(\text{EC}_{50})$ or high background),
89 we included 24,339 patients' samples and 6,590 healthy blood donors' samples in the analysis
90 (Fig. 1A). A titer of $-\log_{10}(\text{EC}_{50}) \geq 1.8$, approximately corresponding to a nominal dilution of $>$
91 $1/64$, was selected as a cutoff to call tau-autoreactive samples (henceforth named $\alpha\tau^+$). Using these
92 parameters, 4.80% ($n=1,169$) of 24,339 patients' samples, but only 1.58% ($n=104$) of 6,590
93 healthy donors were $\alpha\tau^+$ (Fig. 1A-C). These data are indicative of a much higher prevalence of
94 anti-tau immunoreactivity in unselected hospital patients than in healthy individuals ($P<0.001$).

95 Demographic data was available for 4,157 of the 6,590 blood donors included in the study. Their
96 median age was 42 years (interquartile range [IQR] 29-54), whereas the median age of hospital
97 patients was 55 years (IQR: 40-69) ($P<0.001$). Of the healthy blood donors, 40.9% ($n=1,698$) were
98 women, whereas for the hospital group, 47.7% ($n=11,609$) of the patients were women ($P<0.001$).
99 Using a multivariate log-binomial regression model (24, 25) adjusted for age and sex, we found
100 that hospital patients had 2.3 times the risk of healthy donors to be $\alpha\tau^+$ (adjusted RR 2.30, 95%
101 confidence interval (CI) 1.83-2.92, $P<0.001$, Fig. 1D).

102 The replicability of the microELISA screen was evaluated by testing 308 randomly picked samples
103 in duplicate, and was found to be high ($R^2=0.84$, $P<0.001$, Fig. 1E). To estimate any nonspecific
104 cross-reactivity, we determined the immunoreactivity to two other proteins implicated in neuro-
105 degeneration, amyloid- β pyroglutamate and the cellular prion protein (PrP^C) (22). Of 12,297 pa-
106 tient samples, 604 samples were positive against MTBD-tau and 5 against amyloid- β pyrogluta-
107 mate but none was cross-reactive against both targets ($P=1$, χ^2 test) (Fig. 1F). Moreover, of 13,099

108 patient samples, 694 were reactive against MTBD-tau and 15 against PrP^C, but again none was
109 cross-reactive against both targets ($P=0.734$, χ^2 test) (Fig. 1G)

110

111 **Characterization of $\alpha\tau^+$ samples**

112 Anti-tau autoantibodies were purified by MTBD-tau affinity chromatography from four individual
113 $\alpha\tau^+$ patients (P1-P4) and from a pool of six $\alpha\tau^+$ samples for which larger sample volumes were
114 available. Their half-maximal effective concentration (EC_{50}) to MTBD-tau was determined by in-
115 direct ELISA and compared to the EC_{50} of the well-characterized monoclonal anti-MTBD-tau an-
116 tibody, RD4 (dissociation constant $K_d=570$ nM) (26). At equal concentrations, RD4 displayed
117 binding to MTBD-tau with $EC_{50}=0.002$ $\mu\text{g/ml}$ Fig. 2A and no binding to MTBD-tau-free plates,
118 whereas the five purified autoantibody samples had EC_{50} values of 0.042-14.45 $\mu\text{g/ml}$ (Fig. 2A).
119 As expected, no binding to MTBD-tau was observed for the unrelated antibody, Relatlimab (anti-
120 LAG3) (27) (Fig. 2A).

121 To probe the binding specificity of the purified $\alpha\tau^+$ autoantibodies, we performed a soluble-com-
122 petition immunoassay with MTBD-tau (Fig. 2B). This is a stringent assay which, when positive,
123 identifies high-affinity interactions. Purified autoantibodies from four $\alpha\tau^+$ patients and control
124 were pre-incubated with either recombinant MTBD-tau, a pool of eight synthetic 25-meric pep-
125 tides overlapping with each other by 10 residues and covering the MTBD-tau sequence, an unre-
126 lated synthetic 25-meric peptide derived from TREM2 (Triggering Receptor Expressed on Mye-
127 loid Cells 2), or albumin. Each antigen was tested for its capability to impair the binding of purified
128 $\alpha\tau^+$ autoantibodies to plate-bound MTBD-tau by ELISA. Pre-incubation with MTBD-tau and
129 pooled MTBD-tau peptides, but not with the TREM2 peptide or albumin, decreased the ELISA
130 signal in a concentration-dependent manner (Fig. 2C). These results confirm the binding specific-
131 ity of $\alpha\tau^+$ plasma for MTBD-tau.

132 Certain antibodies can display broad polyreactivity which may raise doubts about their specificity.
133 To probe for polyreactivity of purified $\alpha\tau^+$ autoantibodies, we performed indirect ELISA assays
134 against a variety of structurally different unrelated self-antigens and non-self-bacterial antigens,
135 including MTBD-tau, albumin, cardiolipin, DNA, insulin, and lipopolysaccharides (LPS) as well
136 as with uncoated plates. Purified anti-tau autoantibodies were reactive against MTBD-tau but not
137 against any of the tested antigens (Fig. 2D).

138 We then tested the purified $\alpha\tau^+$ autoantibodies by immunofluorescence staining and Western blot-
139 ting. Purified anti-tau autoantibodies staining co-localized to cytoplasmic EGFP-0N4RTau in SH-
140 SY5Y cells and showed similar specific binding to anti-tau mouse monoclonal antibody HT7, but
141 not to non-transfected cells (Fig. 2E). Western blot analysis confirmed that purified $\alpha\tau^+$ autoanti-
142 bodies detected tau-specific bands in cell lysates of SH-SY5Y cells overexpressing tau^{P301L/S320F},
143 but not in wild-type (wt) SH-SY5Y cells (Fig. 2F and Fig. S1). These data provide substantial
144 evidence that the immunoreactivity observed in $\alpha\tau^+$ samples is indeed highly specific for tau.

145 We further investigated the subclass composition of immunoglobulin heavy and light chains of 13
146 $\alpha\tau^+$ plasma samples. All four IgG subclasses were found, with IgG1 being detected in all 13 sam-
147 ples, followed by IgG3 in 12 samples, IgG2 in 11 samples and IgG4 in 8 samples (Fig. 2G). κ light
148 chains were detected in 9 samples and λ light chains in 7 samples (Fig. 2H). Three samples were
149 polytypic for κ and λ (Fig. 2H).

150 We then profiled the epitopes recognized by the MTBD-tau autoantibodies in $\alpha\tau^+$ plasmas and of
151 MTBD-tau affinity chromatography purified autoantibodies from five $\alpha\tau^+$ samples (P2-P6) using
152 a library of 8 synthetic 25-meric peptides with 10 residues of overlap covering the sequence of
153 MTBD-tau. Most samples showed reactivity to peptides 3 (11 of 14) and 5 (10 of 14) which cor-
154 respond to the repeat regions 2 and 3 of MTBD-tau (Figs 2I and S2). A polyclonal antibody re-
155 sponse was identified in at least 7 of 13 samples based on light-chain typing and epitope mapping
156 (Fig. 2G-H). Taken together, these findings confirm the presence of naturally occurring antibodies
157 of different subclasses, light chains and against different epitopes of MTBD-tau in $\alpha\tau^+$ plasma
158 samples.

159

160 **Biological activity of $\alpha\tau^+$ autoantibodies**

161 Anti-tau antibodies can antagonize the aggregation of tau into pathogenic assemblies (28). To in-
162 vestigate whether plasma MTBD-tau autoantibodies interfere with the aggregation of MTBD-tau,
163 MTBD-tau affinity purified autoantibodies from two further $\alpha\tau^+$ samples (P7 and P8) were sub-
164 jected to an *in vitro* tau aggregation assay (28). MTBD-tau aggregation was induced by heparin
165 and shaking and monitored using thioflavin T (ThT) (Fig. 3A). The presence of the anti-MTBD-
166 tau autoantibodies reduced the plateau of the ThT fluorescence signal in the kinetic trace by about
167 half, whereas antibodies purified by protein G affinity chromatography from an $\alpha\tau^-$ patient had no

168 effect (Fig. 3A). These findings indicate that $\alpha\tau^+$ autoantibodies inhibit MTBD-tau aggregation *in*
169 *vitro*

170 Plasma tau is considered a possible biomarker for the progression of several neurological diseases
171 (6-9, 29). To probe for an interference of $\alpha\tau^+$ autoantibodies in plasma tau immunoassays, we
172 added tau⁴⁴¹ to the plasma of healthy donors and examined the effect of $\alpha\tau^+$ autoantibodies onto
173 tau detection (Fig. 3B). Purified anti-MTBD-tau autoantibodies from 5 individual $\alpha\tau^+$ patients (P2-
174 P6) were added to tau⁴⁴¹-spiked plasma. After incubation, the amount of free tau⁴⁴¹ was analyzed
175 by ELISA using the commercial anti-tau BT2 as a capture antibody (epitope on human tau⁴⁴¹:
176 residues 194-198) and ab64193 as a detection antibody (epitope on human tau⁴⁴¹ surrounding res-
177 idue 262 (30)). We observed that purified anti-tau autoantibodies, P4-P6, induced a concentration-
178 dependent impairment of detection of tau⁴⁴¹ (Fig. 3C-D) hampering the detection of plasma-spiked
179 tau⁴⁴¹ by up to approximately tenfold at higher anti-MTBD-tau autoantibodies concentrations (Fig.
180 3C-D). In contrast, P2-P3 did not show any significant impairment of the detection of plasma-
181 spiked tau⁴⁴¹. This variability of interference is explained by the binding epitopes on tau⁴⁴¹. P4-P6
182 occupy tau residues 244 to 282 which include the epitope of the detection antibody ab64193,
183 whereas P2-P3 occupy residues 273 to 327 which are outside the binding epitope of ab64193 (Fig.
184 S2). We thus conclude that the presence of $\alpha\tau^+$ autoantibodies may interfere with the detection of
185 plasma tau in immunoassays depending on the combination of epitopes of the patient samples and
186 of the commercial antibodies used in the immunoassay.

187

188 **Demographic characteristics of tau-immunoreactive patients**

189 We performed univariate logistic regression analyses of basic demographic data available in the
190 electronic health records for the 24,339 hospital patients. The age of $\alpha\tau^+$ patients (median: 58 years;
191 IQR: 43-71) was significantly higher than that of $\alpha\tau^-$ (median: 55; IQR: 40-68; $P < 0.001$, Fig. 4A).
192 A more detailed breakdown of the data showed that the prevalence of $\alpha\tau$ immunoreactivity in-
193 creased with age, from 3.9% in patients aged <29 years to 7.6% in patients older than 90 years
194 ($P < 0.001$, Fig. 4B). A log-binomial regression model (24, 31) estimated that the risk ratio for the
195 presence of anti-MTBD-tau autoantibodies was highest for patients aged 70-99 years (RR 1.26,
196 95%CI 1.11-1.43, $P < 0.001$, Fig. 4C) and for women (RR 1.20, 95%CI 1.07-1.39, $P = 0.002$, Fig.
197 4C). Due to the association of anti-MTBD-tau autoantibodies with increased age and female sex,

198 all further risk ratios were calculated using a multivariate log-binomial regression model adjusted
199 for age and sex [age-and-sex adjusted risk ratio (aRR)].

200 Any possible correlations between α^+ and admission to specific clinical departments might inform
201 on potential associations with specific diseases. The highest age-and-gender adjusted risk ratios
202 for α^+ were found for the departments of angiology (RR 1.84, 95%CI 1.21-2.63, P=0.002) and
203 nephrology (RR 1.50, 95%CI 1.16-1.89, P=0.001, Fig. 4D-E). Importantly, no significant differ-
204 ence was found between the percentage of α^+ and α^- patients from the department of neurology
205 (Fig. 4D).

206

207 **Neurological disorders and anti-tau autoimmunity**

208 We next mined pseudonymized clinical data pertaining to the diagnoses of 23,375 patients as rep-
209 resented by ICD-10 codes (International Classification of Disease and Related Health Problems,
210 10th revision) (Fig. 5A). Given the involvement of tau in neurodegenerative diseases (3), we fo-
211 cused on evaluating the association between anti-MTBD-tau autoantibodies and neurological dis-
212 ease, which we categorized in 23 main groups of disorders. No associations between α^+ and neu-
213 rological diseases were identified (Fig. 5A). To further validate this finding, we performed a tar-
214 geted screen using plasma samples from 47 patients with AD and 68 similarly aged non-AD pa-
215 tients selected from our plasma biobank (Table S1). Samples were tested for anti-MTBD-tau IgG
216 autoantibodies, as in the primary screen, and additionally for anti-MTBD-tau IgA autoantibodies
217 and anti-full-length tau IgG and IgA autoantibodies. No significant difference in reactivity was
218 observed between the plasma samples from AD patients and non-AD controls (Fig. 5B), support-
219 ing the hypothesis that the presence of autoantibodies targeting MTBD-tau is unrelated to AD or
220 other neurological disorders.

221

222 **Systemic disorders and anti-tau autoimmunity**

223 We next assessed possible associations between tau autoimmunity and extraneural diseases, which
224 we binned into 27 main groups of disorders (Fig. 6A). After adjustment for multiple comparisons,
225 α^+ immunoreactivity showed significant associations with vascular disorders (adjusted RR 1.51,
226 95%CI 1.28-1.77, P<0.001), nutritional disorders (adjusted RR 1.31, 95%CI 1.14-1.50, P<0.001),
227 anemia (adjusted RR 1.49, 95%CI 1.21-1.82, P<0.001), kidney disorders (adjusted RR 1.27,
228 95%CI 1.10-1.45, P=0.001) and urinary disorders (adjusted RR 1.40, 95%CI 1.20-1.63, P<0.001)

229 (Fig. 6B), whereas no association was observed among patients with autoimmune disorders (Fig.
230 S3). There was no difference in the coincidence of all comorbidities between the $\alpha\tau^+$ samples (5,
231 0.46%) and the $\alpha\tau^-$ samples (69, 0.33%) ($P=0.633$).

232 To address potential biases arising from grouping and selecting major categories, we further ex-
233 plored the association between $\alpha\tau^+$ and individual ICD-10 codes. Across 276 individual ICD-10
234 codes and after correction for multiple comparisons, eight exhibited significant associations with
235 $\alpha\tau^+$ (Fig. 6B-C). These included “E61 – deficiency of other nutrient elements” (adjusted RR 2.22,
236 95%CI 1.54-3.06, $P<0.001$), “I74 - arterial embolism and thrombosis” (adjusted RR 2.09, 95%CI
237 1.40-2.94, $P<0.001$), “N30 – cystitis” (adjusted RR 1.84, 95%CI 1.32-2.47, $P<0.001$), “I70 – ath-
238 erosclerosis” (adjusted RR 1.57, 95%CI 1.29-1.89, $P<0.001$), “D50 – iron deficiency anemia”
239 (adjusted RR 1.50, 95%CI 1.21-1.82, $P<0.001$), “N39 – other urinary disorders” (adjusted RR
240 1.40, 95%CI 1.19-1.64, $P<0.001$), “B96 – other bacterial agents as the cause of diseases” (adjusted
241 RR 1.40, 95% CI 1.17-1.66, $P<0.001$) and “N18 – chronic kidney disease” (adjusted RR 1.38,
242 95%CI 1.18-1.60, $P<0.001$) (Fig. 6C). Again, it is well-known that many of these diseases are
243 often co-incident in clinical practice. Conversely, we found no significant negative association
244 between tau autoreactivity and any ICD-10 codes that could suggest a decreased risk for a specific
245 disease in $\alpha\tau^+$ patients (Fig. 6B).

246 To further verify the association between $\alpha\tau^+$ and individual ICD-10 codes, we used a different
247 statistical approach. Instead of using a titer of $-\log_{10}(EC_{50}) \geq 1.8$ to dichotomize samples as posi-
248 tives and negatives, we performed a Bayesian logistic regression using logit-transformed EC_{50}
249 values ($-\text{logit}[EC_{50}]$) as a continuous outcome. We could verify that all the previously referred
250 eight ICD-10 codes showed positive associations with $-\text{logit}[EC_{50}]$ (Fig. 6D).

251 With the aim of further validating these conditions as clinically significant associations with
252 plasma MTBD-tau IgG autoantibodies, we examined the association between $\alpha\tau^+$ and 106 com-
253 monly requested laboratory parameters using data available for 24,177 patients. This analysis was
254 independent of any ICD-10 classifiers. After correction for multiple comparisons, the laboratory
255 markers “Leukocytes, urine”, “Potassium” and “Urea” were positively associated with tau auto-
256 immunity (Fig. 6E). The association with increasing levels of urea and potassium suggest a link to
257 kidney failure, whereas leukocytes in urine are a feature of urinary tract infections. These findings
258 are therefore in good agreement and provide a strong independent line of evidence for the hypoth-
259 esis that anti-tau autoimmunity correlates with such disorders.

260 Comparing the prevalence of kidney and urinary disorders in $\alpha\tau^-$ and $\alpha\tau^+$ patients, we identified an
261 excess prevalence of chronic kidney disease of 5.3% in $\alpha\tau^+$ patients (12.4% in $\alpha\tau^-$ and 17.7% in
262 $\alpha\tau^+$), an excess prevalence of cystitis of 1.7% in $\alpha\tau^+$ patients (1.6% in $\alpha\tau^-$ and 3.3% in $\alpha\tau^+$), and an
263 excess prevalence of other urinary disorders of 4.8% (10.3% in $\alpha\tau^-$ and 15.1% in $\alpha\tau^+$) (Fig. 6F).
264 These data further support the hyperprevalence of tau autoimmunity in patients with these diseases.
265

266 **DISCUSSION**

267 Due to their hypothesis-free character and their independence from priors, large-scale seroepide-
268 miological screens have the potential to uncover disease correlations and new biological effects of
269 its targets that may not be discoverable in any other way. Such screens are suited to identifying
270 pathologies correlating with any immunoreactivity, but require economical, massively parallel as-
271 says. Using acoustic dispensing and extensive customized automation, we miniaturized antibody
272 detection to a volume of 3 μ l/sample and to 1,536-well microplates. This allowed us to run 40,000
273 assays/24 hrs using a robotic platform. In total, we performed >300,000 immunoassays on >40,000
274 plasma samples obtained from university hospital patients and healthy blood donors for α τ auto-
275 reactivity (21-23). ELISA miniaturization lowered the cost of individual assays, allowing us to
276 measure eight data points across a dilution range of 1:50 to 1:6,000 for each sample. Consequently,
277 this method enables us to determine autoantibody titers more stringently and unambiguously (21-
278 23).

279 Even after adjustments for age and sex, the α τ ⁺ rate in hospital patients was three-fold higher than
280 in healthy blood donors and was 2.4 times higher than that of autoantibodies targeting other intra-
281 cellular neuronal targets reported by others (32). Plasma α τ IgG correlated with female sex and
282 increased with age. The specificity of α τ ⁺ plasma to MTBD-tau was high and was confirmed by
283 multiple orthogonal assays including epitope mapping. Most α τ ⁺ samples were polyclonal, and all
284 IgG subclasses were represented. Purified α τ autoantibodies exhibited the capability to inhibit
285 MTBD-tau aggregation *in vitro*. Finally, it was possible to compete them by MTBD-tau and a pool
286 of synthetic MTBD-tau peptides, but not by other antigens.

287 The much higher prevalence of α τ positivity in hospital patients than in healthy blood donors sug-
288 gests that tau autoreactivity is low in healthy populations and that α τ autoantibodies are associated
289 with disease. However, we did not find any association between α τ ⁺ and any neurological condi-
290 tions including neurodegenerative diseases. This observation is compatible with reports of similar
291 levels of plasma tau autoantibodies in Alzheimer's disease patients and non-demented controls
292 (33). Instead, we uncovered a robust and specific association between plasma anti-MTBD-tau IgG
293 autoantibodies and the diagnosis of kidney and urinary disorders, which was validated by the in-
294 dependent finding of association between α τ immunoreactivity and higher prevalence of positive

295 samples from the department of Nephrology, grouped kidney and urinary diseases, individual kid-
296 ney and urinary diagnosis codes as well as high serum urea and potassium and high urine leuko-
297 cytes, which are clinical laboratory biomarkers of kidney and urinary disorders.

298 This seroepidemiological studies cannot establish causality: hence $\alpha\tau$ seropositivity could be a
299 cause or a consequence of the clinical syndromes associated with it. Indeed, some patients with
300 frontotemporal dementia and Parkinsonism caused by mutant tau experience urinary incontinence
301 (34) which may plausibly result from neuronal pathologies. However, tau is expressed in extraneu-
302 ral tissues, including kidney podocytes and urinary bladder (2, 35-37), and its ablation causes glo-
303 merular pathologies (38). Besides raising the possibility that plasma $\alpha\tau$ autoantibodies might drive
304 kidney pathologies, these findings suggest that such autoantibodies represent useful biomarkers of
305 these diseases. Finally, these findings suggest that it will be important to monitor renal and urinary
306 function in the current clinical trials of tau immunotherapy (39-41).

307 Recent studies have explored the use of total and phosphorylated tau measurements in plasma as
308 biomarkers for AD diagnosis and for monitoring its progression (6-9, 29, 42-46). Measurement of
309 plasma tau levels may enter regular clinical use as an easily accessible biomarker of AD. However,
310 we found that anti-MTBD-tau autoantibodies could hinder tau detection in plasma by binding to
311 epitopes recognized by commercial biomarker immunoassays. This aligns with prior research in-
312 dicating that both plasma anti-tau autoantibodies and administered anti-tau antibodies can influ-
313 ence the dynamics of tau levels in plasma (47). Additionally, a recent community cohort study
314 using an immunoassay for AD screening revealed associations between plasma tau levels and nu-
315 merous comorbidities, with chronic kidney disease showing one of the strongest associations (48).
316 These results imply that the presence of anti-tau autoantibodies in plasma might impact the effec-
317 tiveness of plasma tau as an AD biomarker, particularly for patients with kidney or urinary dis-
318 eases. This consideration may become crucial as plasma tau levels move toward routine clinical
319 use in AD diagnosis.

320 Our large-scale assessment of plasma tau autoimmunity has certain limitations. Firstly, most sam-
321 ples analyzed in our study came from a university hospital cohort, implying a bias towards com-
322 plex pathologies and polymorbidities. To account for this, we included a vast collection of samples
323 from healthy blood donors. Secondly, our study is confined to two sites within a single region with
324 approximately 1,500,000 inhabitants whose ethnic composition was not thoroughly examined. Ad-
325 ditionally, a direct comparison of the prevalence of plasma anti-tau antibodies in these two cohorts

326 may potentially suffer from variations in materials, collection methods, and handling processes at
327 the two different sites. Thirdly, our study is restricted to the analysis of specific disease groups and
328 the absence of a longitudinal disease cohort that would allow for examining a time course, origin,
329 and causal role of these autoantibodies. Finally, we used bacterially expressed MTBD-tau as target,
330 thereby excluding full-length or post-translationally modified tau epitopes. As a result, plasma
331 anti-tau autoantibodies associated with AD pathology might be missed, and our methodology may
332 underestimate the prevalence of total anti-tau autoantibodies.

333 In conclusion, our study found a high seroprevalence of anti-MTBD-tau IgG autoantibodies in
334 both plasma samples from university hospital patients and healthy blood donors. Tau autoimmun-
335 ity is associated with female sex, older age and previously unrecognized extraneural diseases.
336 These findings point to unrecognized roles for tau and anti-tau autoantibodies in extraneural pa-
337 thologies and call for attentive clinical monitoring of such diseases in clinical trials of tau-targeting
338 therapies and in the use of plasma tau as a biomarker of disease.

339

340 MATERIALS AND METHODS

341 Study design

342 Collection of samples and clinical data were conducted according to study protocols approved by
343 the Cantonal Ethics Committee of the Canton of Zurich, Switzerland (KEK-ZH Nr. 2015-0561,
344 BASEC-Nr. 2018-01042, and BASEC-Nr. 2020-01731). From December 2017 until February
345 2020, residual heparin plasma samples were obtained from the Department of Clinical Chemistry,
346 University Hospital of Zurich), Switzerland. Blood samples were collected during routine clinical
347 care from patients admitted either as inpatients or outpatients and were only included if basic de-
348 mographic data was available, age was ≥ 18 years, and an informed consent for research had been
349 provided. From March until July 2020, EDTA plasma samples were obtained from the Blood Do-
350 nation Center of Zurich, Switzerland from blood donors according to standard criteria of blood
351 donation. Exclusion criteria were as shown previously (21). Plasma samples were biobanked in
352 384-well plates at the Institute of Neuropathology, University of Zurich and tested on an automated
353 indirect microELISA high-throughput platform for natural IgG autoantibodies against the micro-
354 tubule-binding-domain of tau (MTBD-tau, tauK18, for details see (21, 22) and below).

355 Demographic and clinical data for the hospital cohort was obtained from clinical electronic records
356 of the University Hospital of Zurich with follow-up until December 2021, while detailed clinical
357 data for the blood donor cohort were not available for this study.

358 For the AD targeted screen, the AD patients and non-neurodegeneration controls were selected
359 from the biobank of samples at the Institute of Neuropathology, USZ, using *International Statis-
360 tical Classification of Diseases and Related Health Problems, Tenth Revision* (ICD-10) codes. AD
361 patients were defined using ICD-10 code F00 or G30 and non-neurodegeneration controls were
362 defined by the lack of any Fxx or Gxx ICD-10 codes.

363 Automated microELISA screen

364 Plasma samples were tested for natural anti-MTBD-tau IgG autoantibodies in a microELISA
365 screen (21-23). Briefly, high-binding 1,536-well plates (Perkin Elmer, SpectraPlate 1536 HB)
366 were coated with 1 $\mu\text{g/mL}$ of in-house produced MTBD-tau (see protocol below) at 37 °C for 60
367 min. Plates were washed 3x with phosphate-buffered saline 0.1% Tween@20 (PBST) using a Bi-
368 otek El406 washer-dispenser. Plates were blocked for 90 min with 5% milk (Migros) in PBST.
369 Plasma was diluted 1:20 in 1% milk in PBST and dispensed into the MTBD-tau-coated plates
370 using ultrasound dispensing with an ECHO 555 Liquid Handler (Labcyte/Beckman Coulter) and

371 in different volumes to a final volume of 3 μ L/well and testing each sample at eight serial two-fold
372 dilutions (1:50 to 1:6,000). Human IgG-depleted serum (MyBioSource) was used as negative con-
373 trol and anti-tau RD4 (4-repeat isoform) mouse monoclonal antibody (05-804 clone 1E1/A6 Merck
374 Millipore) as a positive control. Samples were incubated for 120 min at room temperature (RT)
375 after which plates were washed 5x with PBST. Secondary antibody peroxidase AffiniPure® goat
376 anti-mouse IgG H+L (115-035-003, Jackson ImmunoResearch) at 1:2,000 dilution in 1% milk
377 PBST for the RD4 positive control, and peroxidase AffiniPure® goat anti-human IgG Fc γ -specific
378 (109-035-098, Jackson ImmunoResearch) 1:4,000 dilution in 1% milk PBST for the plasma sam-
379 ples and the IgG-depleted serum negative control were dispensed into the plates using a Biotek
380 MultifloFX dispenser. Secondary antibodies were incubated for 60 min at RT after which plates
381 were washed 3x with PBST. 3,3',5,5'-Tetramethylbenzidine (TMB) Chromogen Solution for
382 ELISA (Invitrogen) was added to the plates as colorimetric horseradish peroxidase (HRP) sub-
383 strate and incubated for 3 min at RT. Finally, 0.5 M H₂SO₄ was added to stop the reaction. Plates
384 were briefly centrifuged after each dispensing step except after dispensing of TMB. Plates were
385 read at Optical Density (OD) = 450 nm in a plate reader (Perkin Elmer, Envision).

386 For the replicability assessment, 308 samples were tested in duplicates using the same protocol as
387 described before, and running the replicates on the same day but using different 1536-well assay
388 (destination) plates, different plate coordinates for each replicate, and calculating the $-\log_{10}(\text{EC}_{50})$
389 of each replicate independently.

390 Non-specific cross-reactivity was assessed by testing plasma samples against against-MTBD-tau
391 and amyloid- β pyroglutamate (13,099 hospital patients' plasma samples) and the cellular prion
392 protein (PrP^C) (12,297 hospital patients' samples) using a similar protocol as described above.

393 **Production and purification of recombinant tau**

394 The gene encoding the human truncated 4R-tau corresponding to the microtubule binding domain
395 of tau protein (MTBD-tau) was cloned into a pRSET-A plasmid (Invitrogen). For protein expres-
396 sion the respective vector was transformed into *E.coli* BL21(DE3) cells. Bacterial cells were grown
397 in Luria Broth (LB) medium (Invitrogen) at 37 °C until an OD₆₀₀ of 0.8 was reached and were then
398 induced with isopropyl- β -D-thiogalactoside (IPTG) at a final concentration of 1 mM. After grow-
399 ing the cells for additional 6 h at 37 °C, cultures were harvested by centrifugation (6,000g, 10 min,
400 4 °C). Pellets were suspended in 20 mM piperazine-N,N-bis(2-ethanesulfonic) acid (PIPES), pH
401 6.5, 1 mM ethylenediaminetetraacetic acid (EDTA) and 50 mM 2-mercaptoethanol buffer and

402 sonicated for 30 min at 4 °C. NaCl to 500 mM final concentration was added, samples were boiled
403 at 95 °C for 20 min and centrifuged (9,000g, 30min, 4 °C). Ammonium sulfate was slowly added
404 to a final concentration of 55% m/v and stirred for 1 h at room temperature (RT). Samples were
405 centrifuged (15,000g, 10min, 4 °C), pellets were resuspended in 20 mM 4-(2-hydroxyethyl)piper-
406 azine-1-ethanesulfonic acid (HEPES) (pH 7.0), 2 mM dithiothreitol (DTT), passed through a 0.45
407 µm Acrodisc® filter (Sigma) and loaded onto Sepharose SP Fast Flow resin (Cytiva). Tau was
408 eluted using a linear salt gradient from 0 to 1 M NaCl in 20 mM HEPES, pH 7.0, 2 mM DTT.
409 Fractions containing tau were concentrated using Amicon® Ultra-15 centrifugal filter unit (10-
410 kDa MWCO) (Merck) and dialyzed overnight at 4°C against phosphate-buffered saline (PBS) (pH
411 7.4) (Kantonsapotheke Zurich), 1mM DTT. Pooled samples were passed through a HiLoad 26/60
412 Superdex75 (GE Healthcare) column. Protein samples were analyzed by SDS-PAGE and samples
413 containing tau were concentrated using an Amicon® Ultra-15 centrifugal filter unit (10-kDa
414 MWCO). Samples were assessed by SDS-PAGE and electrospray ionization-mass spectrometry
415 (Functional Genomics Center Zurich, Switzerland). Pure MTBD-tau samples were stored until
416 further use at -80°C. The concentration of tau was determined using a bicinchoninic acid assay
417 (Pierce BCA Protein Assay Kit, Thermo Fisher).

418 For the purification of full-length tau, a similar protocol was used with the following changes. The
419 gene encoding the longest 4R isoform of human full-length tau protein, tau⁴⁴¹, (tau/pET29b,
420 Addgene #16316, gift from Peter Klein (49)) was cloned into a pRSET-A plasmid (Invitrogen).
421 For protein expression, *E.coli* BL21(DE3)pLysS cells were transformed with the pRSET-A plas-
422 mid encoding tau⁴⁴¹. Cells were grown in Overnight Express™ Instant TB media (Novagen) for 6
423 h at 37 °C and then 12 h at 25 °C. Fractions containing full-length tau were concentrated using
424 Amicon® Ultra-15 centrifugal filter unit (30-kDa MWCO) (Merck).

425 **Purification of anti-tau autoantibodies from patient samples**

426 Heparin plasma (between 3 mL and 20 mL per hospital cohort patient) was diluted 1:3.3 in PBS,
427 and centrifuged (6,000 g, 10 min, 4 °C). The supernatant was loaded on a column containing 3 mL
428 of epoxy-MTBD-tau (prepared with a previous overnight incubation of MTBD-tau and epoxy resin
429 in a binding buffer of 0.1 M NaH₂PO₄-NaOH, 1 M NaCl, pH 9.2) by repetitive loading of the
430 plasma sample overnight at 4 °C. The column was washed with 50 mL of PBS, and MTBD-tau
431 autoantibodies were eluted four times with 5 mL 0.1 M glycine-HCl, pH 2.5, and immediately
432 neutralized to pH 7.0 with 1 M Tris-HCl. Fractions containing antibodies against MTBD-tau were

433 identified using an indirect colorimetric ELISA. Fractions containing the eluted antibodies were
434 stepwise concentrated using Amicon® Ultra-15, Ultra-4, and Ultra-0.5 mL centrifugal filter units
435 (50-kDa MWCO) to up to a volume of 1 mL.

436 **Competitive ELISAs**

437 For the competitive ELISAs of MTBD-tau autoantibodies, high-binding 384-well plates (Perkin
438 Elmer, SpectraPlate 384 HB) were coated with 20 µL of 0.5 µg/mL of MTBD-tau at 4 °C over-
439 night. Afterwards, plates were washed 3x with PBST with a Biotek El406 washer dispenser and
440 blocked with 5% SureBlock™ (Lubio) in PBST for 120 min. Purified autoantibodies from hospital
441 cohort patients' plasma were diluted 1:50 in 1% SureBlock™ (Lubio) in PBST (sample buffer).
442 Anti-tau RD4 mouse monoclonal antibody (05-804 clone 1E1/A6 Merck Millipore) was diluted to
443 a final concentration of 0.4 µg/mL. Bovine serum albumin (Thermo Scientific), in house purified
444 recombinant MTBD-tau, a pool of eight synthetic peptides covering the sequence of MTBD-tau
445 with 25 amino acids length and 10 amino acids of overlap (Genscript) and an unrelated 25 amino
446 acid length synthetic TREM2 (Triggering receptor expressed on myeloid cells 2) peptide
447 (GenScript) were used as competing antigens. Antibody samples were incubated overnight at 4°C
448 with serial 2-fold dilutions of antigens solutions in sample buffer from 20,000 nM to 2.44 nM final
449 concentration. Antibody-antigen solutions were added to the plates and incubated for 45 min at
450 RT. Plates were washed 3x with PBST using a Biotek El406 washer dispenser and secondary
451 antibodies were added as follows: peroxidase AffiniPure® goat anti-Human IgG (H+L) (109-035-
452 088, Jackson ImmunoResearch) diluted 1:3,000 and peroxidase AffiniPure® goat anti-mouse IgG
453 H+L (115-035-003, Jackson ImmunoResearch) diluted 1:2,000. Secondary antibodies were incu-
454 bated for 60 min at RT and then plates were washed plates 4x with PBST. TMB Chromogen So-
455 lution for ELISA (Invitrogen) was added to the plates and incubated for 7 min at RT. Finally, 0.5
456 M H₂SO₄ was added. Plates were briefly centrifuged after each dispensing step except after dis-
457 pensing colorimetric substrate. Plates were read at OD = 450 nm in a plate reader (SpectraMax®
458 Paradigm®, Molecular Devices).

459 For the competitive sandwich ELISAs for the detection of tau in plasma, a similar approach was
460 applied with several changes. High-binding 384-well plates (Perkin Elmer, SpectraPlate 384 HB)
461 were coated with 4 µg/mL BT2 tau monoclonal antibody (epitope on human tau, RSGYS, between
462 residue 194 and 198) (#MN1010, Thermo Fisher) in PBS. Samples were diluted in sample buffer
463 as follows: recombinant human tau⁴⁴¹ (rPeptide) was diluted to a final concentration of 0.015

464 ng/mL and incubated with purified anti-tau autoantibodies four-fold serially diluted (1:1.66 to
465 1:106.6) in 1:2 plasma for 120 min at 37°C with rotation at 500 rpm. Samples were transferred to
466 BT2 antibody-coated plates and incubated for 45 min at RT. Plates were then washed 4x with
467 PBST and ab64193(epitope Ser262 on non-phosphorylated and phosphorylated of human tau) pol-
468yclonal IgG antibody (Abcam) at 0.125 µg/mL was incubated for 45 min at RT. Plates were
469 washed 4x with PBST and peroxidase AffiniPure® goat anti-Rabbit IgG (H+L) (111-035-045,
470 Jackson ImmunoResearch) diluted 1:2,000 was incubated 60min at RT. Plates were washed plates
471 4x with PBST, and 1-Step™ Ultra TMB-ELISA solution (Thermo Fisher) was incubated for 7 min
472 at RT. After addition of 0.5 M H₂SO₄, plates were read at OD = 450 nm in a plate reader (Perkin
473 Elmer, Envision).

474 **Indirect ELISAs**

475 To test for polyreactivity, purified anti-tau autoantibodies were tested by indirect ELISA against
476 several antigens (50, 51). High-binding 384-well plates (Perkin Elmer, SpectraPlate 384 HB) were
477 coated with 1 µg/mL of in house purified MTBD-tau in PBS, 10 µg/mL of double stranded DNA
478 from calf-thymus (Sigma) in PBS, 10 µg/mL of lipopolysaccharides from *E.coli* O111:B4 (Sigma)
479 in PBS, 5 µg/mL of human recombinant insulin (Sigma) in PBS, 10 µg/mL of bovine serum albu-
480min (Thermo Fisher) in PBS, 2 µg/mL of cardiolipin solution from bovine heart (Sigma) in ethanol
481 or left high-binding plates uncoated at 4 °C overnight. Plates were washed 3x with PBST using a
482 Biotek El406 washer dispenser and then blocked 5% SureBlock™ (Lubio) in PBST for 120 min
483 at RT. The following samples serially diluted 1:1 in sample buffer were incubated for 120 min at
484 RT: patient purified anti-tau autoantibodies were diluted 1:33, human IgG-depleted plasma (Bio-
485 Source) was 1:50 diluted and used as a negative control, anti-DNP (Sigma) was diluted to a final
486 concentration of 6 µg/mL and used as a positive control for cardiolipin, DNA and albumin coated
487 plates, anti-tau RD4 mouse monoclonal antibody (05-804 clone 1E1/A6 Merck Millipore) was
488 diluted to a final concentration of 6 µg/mL and used as a positive control for MTBD-tau coated
489 plates, pooled plasma from 20 patients (Institute Clinical Chemistry (IKC), University Hospital
490 Zurich) was diluted 1:25 and used as a positive control for insulin, lipopolysaccharides and un-
491 coated plates. Plates were then washed 4x with PBS-T using a Biotek El406 washer dispenser.
492 Secondary antibodies were diluted and incubated for 60 min at RT as follows: peroxidase Affini-
493 Pure® goat anti-human IgG (H+L) (109-035-088, Jackson ImmunoResearch) diluted 1:3,000 and
494 added to purified MTBD-tau autoantibodies and IKC pool wells, peroxidase AffiniPure® goat

495 anti-mouse IgG H+L (115-035-003, Jackson ImmunoResearch) diluted 1:2,500 and added to anti-
496 RD4 wells, and peroxidase AffiniPure® goat anti-rabbit IgG (H+L) (111-035-045, Jackson Im-
497 munoResearch) diluted 1:4,000 and added to anti-DNP wells. Plates were washed plates 4x with
498 PBST. TMB Chromogen solution for ELISA (Invitrogen) was incubated for 7 min at RT. Finally,
499 0.5 M H₂SO₄ was added. Plates were briefly centrifuged after each dispensing step except after
500 dispensing colorimetric substrate. Plates were read at OD = 450nm in a plate reader (SpectraMax®
501 Paradigm®, Molecular Devices).

502 For relative affinity measurements, we used a similar approach with the following modifications.
503 An indirect ELISA in 384-well plates (Perkin Elmer, SpectraPlate 384 HB) with MTBD-tau as a
504 coating antigen, was used. The starting concentration of all antibodies, assayed in triplicates, was
505 10 µg/mL. They were successively diluted 1:3 to reach a concentration of 2x10⁻⁶ µg/mL. As ref-
506 erence antibody, we used purified RD4 kindly provided by Prof. Rohan de Silva (UCL Queen
507 Square Institute of Neurology, London, UK). As additional controls, we used anti-LAG3 (Lym-
508 phocyte Activation Gene 3) antibody Relatlimab (27), ατ plasma sample and uncoated plates. The
509 respective EC₅₀ values were determined using logistic regression, as described below.

510 For IgG subclassing, the following secondary antibodies were used: rabbit anti-human IgG1 (SA5-
511 10202, Invitrogen), rabbit anti-human IgG2 (SA5-10203, Invitrogen), rabbit anti-human IgG3
512 (SA5-10204, Invitrogen) or rabbit anti-human IgG4 (SA5-10205, Invitrogen) diluted 1:1,500, pe-
513 roxidase AffiniPure® goat anti-rabbit IgG (H+L) antibody (111-035-045, Jackson Immu-
514 noResearch) diluted 1:2,500.

515 For immunoglobulin light chain typing, the following secondary antibodies were used: peroxidase
516 goat anti-human κ (22) 1:4,000 diluted, peroxidase goat anti-human λ (22) 1:4,000 diluted.

517 For epitope mapping, a similar approach was used: high-binding 384-well plates (Perkin Elmer,
518 SpectraPlate 384 HB) with 1 µg/mL of each individual MTBD-tau synthetic peptide (GenScript)
519 diluted in PBS at 4 °C overnight. 8 synthetic peptides spanning the sequence of MTBD-tau with
520 25 amino acids length and 10 amino acids of overlap were used. Plasma samples were diluted 1:50,
521 human IgG-depleted serum (MyBioSource) was 1:50 diluted and used as a negative control and
522 anti-tau RD4 mouse monoclonal antibody (05-804 clone 1E1/A6 Merck Millipore) was diluted to
523 a final concentration of 6 µg/mL and used as a positive control. The following secondary antibod-
524 ies diluted in sample buffer were used: peroxidase AffiniPure® goat anti-human IgG (H+L) (109-

525 035-088, Jackson ImmunoResearch) diluted 1:5,000 and peroxidase AffiniPure® goat anti-mouse
526 IgG H+L (115-035-003, Jackson ImmunoResearch) diluted 1:2,500 and added to anti-RD4 wells.

527 ***In vitro* MTBD-tau aggregation assay**

528 MTBD-tau *in vitro* aggregation experiments were performed as previously described (28). Briefly,
529 7 μM of in house purified recombinant MTBD-tau, 3.5 μM of heparin (Santa Cruz Biotechnology)
530 and 10 μM of thioflavin T (ThT, Sigma) were diluted in PBS. The patient purified anti-tau auto-
531 antibodies and controls (plasma sample reactive against the LAG3 and IgG-purified using Protein
532 G Sepharose (Cytiva)) were added at the indicated apparent stoichiometries in Fig. 3A and the
533 mixtures with a total volume of 200 μl were added to black 96-well polystyrene microplates (Nunc,
534 Prod. No. 265301). Measurements of ThT fluorescence (450/480 nm ex/em filters; bottom read
535 mode) were performed at 37°C under continuous orbital shaking (425 cpm) every 15 min for 96 h
536 in a FLUOstar Omega microplate reader (BMG Labtech).

537 **Western blotting**

538 SH-SY5Y wild-type cells (Sigma) and SH-SY5Y cells overexpressing double-mutant tau^{P301L/S320F}
539 were lysed in 0.5% Triton™ X-100 (Sigma Aldrich) in PBS, supplemented with cComplete™ Mini
540 EDTA-free Protease Inhibitor Cocktail (Roche) on ice and supernatant was recovered after cen-
541 trifugation (14,000g, 20min, 4°C). Protein concentration was estimated using a bicinchoninic acid
542 assay (Pierce BCA Protein Assay Kit, Thermo Fisher) and sample volumes were adapted to 30 μg
543 of total protein. Samples were loaded onto NuPAGE 12% Bis-Tris gels (Invitrogen). Gels were
544 loaded in the following repeating pattern: protein ladder, SH-SY5Y wt and SH-SY5Y tau^{P301L/S320F}
545 cell lysates. SDS-PAGE gels were run at 180 V in MES buffer for 45 min, transferred to nitrocel-
546 lulose membranes (Invitrogen) using a dry transfer system (iBlot 2 Gel Transfer Device, Invitro-
547 gen, Thermo Fisher), membranes were cut vertically along the protein ladder and blocked with 5%
548 SureBlock (Lubio Science) in PBST for 30 min at RT. Membranes were incubated with patient
549 purified anti-tau autoantibodies 1:100 diluted in in 1% SureBlock in PBST overnight at 4 °C. Neg-
550 ative control membranes were not incubated with primary antibodies. Membranes were washed
551 3x for 5 min with PBST and then incubated with the following secondary antibodies for 60 min at
552 RT: peroxidase AffiniPure® goat anti-mouse IgG H+L (115-035-003, Jackson ImmunoResearch)
553 1:10,000 and peroxidase AffiniPure® goat anti-human IgG (H+L) (109-035-088, Jackson Immu-
554 noResearch) 1:10,000 diluted with 1% SureBlock in PBST. The negative control was only incu-
555 bated with peroxidase goat anti-human secondary antibody. Monoclonal mouse anti-actin clone

556 C4 (MAB1501R, Chemicon) diluted 1:10,000 in 1% SureBlock in PBST was used as a loading
557 control. Membranes were washed 4x for 5 min with PBST and developed using the Immobilon
558 Crescendo HRP Substrate (Millipore). Individual membranes were imaged using the Fusion SOLO
559 S imaging system (Vilber).

560 **Immunofluorescence studies**

561 SH-SY5Y cells were transiently transfected with EGFP-0N4Rtau, using a Lipofectamine™ 2000
562 (Invitrogen) according to manufacturer's protocol and a pRK5 plasmid encoding EGFP-0N4RTau
563 (Addgene #46904, kind gift from Dr. Karen Ashe (52)), a human four-repeat isoform of tau tagged
564 with enhanced green fluorescent protein (EGFP) at the N-terminus. After 48 h cells were fixed
565 with 4% paraformaldehyde, permeabilized with 0.5% BSA, 0.1% Triton™ X-100 in PBS for 20
566 min at RT and blocked with 0.5% BSA in PBS for 60 min at RT. Primary antibodies were incu-
567 bated for 60 min at RT diluted in 0.5% BSA in PBS as follows: purified anti-tau autoantibodies
568 were diluted 1:25, tau mouse monoclonal antibody HT7 (MN1000, Thermo Fisher) diluted 1:500
569 and used as a positive control. Negative controls were not incubated with primary antibodies. Cells
570 were washed 3x with 0.5% BSA in PBS and incubated 30 min at RT as follows: for HT7 stains
571 with goat anti-mouse IgG (H+L) cross-adsorbed Alexa Fluor™ 555 (A-21422, Invitrogen) diluted
572 1:500 and counterstained with 4,6-diamidino-2-phenylindole (DAPI) 1mg/mL (Thermo Fisher)
573 diluted 1:10,000 in 0.5% BSA in PBS, and for purified anti-tau autoantibodies and negative con-
574 trols with biotin AffiniPure® goat anti-human IgG (H+L) (109-065-003, Jackson Immu-
575 noResearch) diluted 1:200 in 0.5% BSA in PBS. For purified anti-tau autoantibodies and negative
576 controls, cells were further incubated for 30 min at RT with streptavidin Alexa Fluor™ 594 con-
577 jugate diluted 1:200 and counterstained with DAPI diluted 1:10,000 in 0.5% BSA in PBS. Before
578 mounting on glass sides, cells were washed cells 2x for 3 min in 0.5% BSA in PBS. Cells were
579 mounted on glass slides with Fluorescence Mounting Medium (Dako) and imaged with a TCS SP5
580 confocal laser scanning microscope (Leica). Imaging was performed with equipment from the
581 Center for Microscopy and Image Analysis, University of Zurich.

582 **Statistical analysis**

583 Negative logarithm half-maximal response, or “log₁₀(EC₅₀)” values, were determined by fitting
584 the OD = 450nm of the eight dilution points of each sample tested in the automated microELISA
585 to a logistic regression fitter (21). Samples with a mean squared residual error >20% of the
586 log₁₀(EC₅₀) were classified as non-fittable and were not included in the analysis, as shown before

587 (22). We used $-\log_{10}(\text{EC}_{50})$ as a surrogate of antibody titers and classified as positives/ $\alpha\tau^+$ the
588 samples with a high $-\log_{10}(\text{EC}_{50})$, using a cut-off of $-\log_{10}(\text{EC}_{50}) \geq 1.8$ for the high-throughput
589 screen. In cases where more than one sample was available for the same individual the most recent
590 $\log_{10}(\text{EC}_{50})$ value was used.

591 Demographic features were available for the hospital cohort as well as the blood donors' cohort.
592 Age is presented as median with interquartile range and comparisons were performed using non-
593 parametric Mann-Whitney U test. Categorized age groups and sex of positive and negative are
594 shown as percentages and compared using two-proportions Z-test or χ^2 test for trend in proportions
595 as indicated. We used log-binomial regression models (24, 53) to investigate the association be-
596 tween the detection of anti-MTBD-tau IgG autoantibodies and different demographic features.
597 Risk ratios and 95% confidence intervals were calculated using MTBD-tau autoreactivity as a
598 binomial outcome.

599 Log-binomial regression models used MTBD-tau-autoreactivity as a binomial outcome and were
600 adjusted for age and sex allowing the estimation of age-and-sex adjusted risk ratios and 95% con-
601 fidence intervals. For the exploration of the association between MTBD-tau-autoreactivity and
602 neurological disorders, we used multivariate log-binomial regression models to estimate age-and-
603 sex adjusted risk ratios and 95% confidence intervals using 23 major groups of ICD-10 codes
604 (Supplementary Table S2) corresponding to the neurological disorders identified at least once in
605 the positive samples. For the AD cohort ELISA screen, $\log_{10}(\text{EC}_{50})$ values were compared using
606 Mann-Whitney U test.

607 For the exploration of the association between MTBD-tau-autoreactivity and systemic disorders,
608 we used multivariate log-binomial regression models to estimate age-and-sex adjusted risk ratios
609 and 95% confidence intervals using 27 major groups of ICD-10 codes (Supplementary Table S3)
610 or 276 individual ICD-10 codes corresponding to systemic disorders identified at least once in the
611 positive samples and with at least 200 total counts to avoid overinterpretation of rare cases of
612 disease. Individual disease entities with a P value < 0.05 Bonferroni corrected for multiple com-
613 parisons were included in a multivariate log-binomial regression analysis. In addition, we con-
614 ducted a Bayesian logistic regression as described recently (21, 54-56), using $-\text{logit}_{10}(\text{EC}_{50})$ values
615 as outcome, i.e. without dichotomising the outcome using the R package rstanarm and the follow-
616 ing priors (prior=normal[0, 2.5, autoscale=TRUE], prior_intercept = normal[5000, 2.5, au-
617 toscale=TRUE]) prior_aux = exponential [1, autoscale =TRUE]. We thereby aimed to confirm the

618 positive association between ICD-10 codes previously identified using a conventional logistic re-
619 gression model with high $-\log_{10}(EC_{50})$ values. Each ICD-10 code was analyzed in an independent
620 logistic regression and adjusted for age and sex.

621 For the exploration of the association between MTBD-tau-autoreactivity and clinical laboratory
622 parameters, we used laboratory parameters with more than 2,000 total counts and calculated me-
623 dian values of the total values available for each patient in case of repetition of the clinical labor-
624 atory test. We used multivariate log-binomial regression models to estimate age-and-sex adjusted
625 risk ratios and 95% confidence intervals using 106 clinical laboratory tests.

626 Throughout the manuscript, statistical significance was defined by 2-tailed P value ≤ 0.05 . P values
627 were corrected for multiple comparisons using Bonferroni's method when applicable as described
628 in each Figure/Table.

629 For IgG subclassing, immunoglobulin light chain typing and epitope mapping experiments, we
630 classified samples to be reactive if the OD_{450} was higher than the average of all negatives $OD_{450} +$
631 $2x$ the standard deviation of the OD_{450} of the negatives.

632 For the MTBD-tau aggregation experiments, the mean baseline fluorescence values were sub-
633 tracted from the mean fluorescence values at each time point which were then normalized to max-
634 imum baseline-subtracted fluorescence values and multiplied by 100 (57).

635 Statistical analyses and data visualization were performed using R version 4.3.2 and RStudio ver-
636 sion 1.4.1106 (58).

637 **List of Supplementary Materials:**

638 Table S1, S2 and S3

639 Fig. S1, S2 and S3

640

641 References

- 642 1. Y. Gu, F. Oyama, Y. Ihara, Tau is widely expressed in rat tissues. *J Neurochem* **67**, 1235-
643 1244 (1996).
- 644 2. M. Uhlen, L. Fagerberg, B. M. Hallstrom, C. Lindskog, P. Oksvold, A. Mardinoglu, A.
645 Sivertsson, C. Kampf, E. Sjostedt, A. Asplund, I. Olsson, K. Edlund, E. Lundberg, S. Navani,
646 C. A. Szigyanto, J. Odeberg, D. Djureinovic, J. O. Takanen, S. Hober, T. Alm, P. H. Edqvist,
647 H. Berling, H. Tegel, J. Mulder, J. Rockberg, P. Nilsson, J. M. Schwenk, M. Hamsten, K. von
648 Feilitzen, M. Forsberg, L. Persson, F. Johansson, M. Zwahlen, G. von Heijne, J. Nielsen, F.
649 Ponten, Proteomics. Tissue-based map of the human proteome. *Science* **347**, 1260419
650 (2015).
- 651 3. K. S. Kosik, C. L. Joachim, D. J. Selkoe, Microtubule-associated protein tau (tau) is a major
652 antigenic component of paired helical filaments in Alzheimer disease. *Proc Natl Acad Sci*
653 *U S A* **83**, 4044-4048 (1986).
- 654 4. C. L. Joachim, J. H. Morris, K. S. Kosik, D. J. Selkoe, Tau antisera recognize neurofibrillary
655 tangles in a range of neurodegenerative disorders. *Ann Neurol* **22**, 514-520 (1987).
- 656 5. B. J. Hanseeuw, R. A. Betensky, H. I. L. Jacobs, A. P. Schultz, J. Sepulcre, J. A. Becker, D. M.
657 O. Cosio, M. Farrell, Y. T. Quiroz, E. C. Mormino, R. F. Buckley, K. V. Papp, R. A. Amariglio,
658 I. Dewachter, A. Ivanoiu, W. Huijbers, T. Hedden, G. A. Marshall, J. P. Chhatwal, D. M.
659 Rentz, R. A. Sperling, K. Johnson, Association of Amyloid and Tau With Cognition in
660 Preclinical Alzheimer Disease: A Longitudinal Study. *JAMA Neurol* **76**, 915-924 (2019).
- 661 6. N. Mattsson, H. Zetterberg, S. Janelidze, P. S. Insel, U. Andreasson, E. Stomrud, S.
662 Palmqvist, D. Baker, C. A. Tan Hehir, A. Jeromin, D. Hanlon, L. Song, L. M. Shaw, J. Q.
663 Trojanowski, M. W. Weiner, O. Hansson, K. Blennow, A. Investigators, Plasma tau in
664 Alzheimer disease. *Neurology* **87**, 1827-1835 (2016).
- 665 7. S. Janelidze, N. Mattsson, S. Palmqvist, R. Smith, T. G. Beach, G. E. Serrano, X. Chai, N. K.
666 Proctor, U. Eichenlaub, H. Zetterberg, K. Blennow, E. M. Reiman, E. Stomrud, J. L. Dage,
667 O. Hansson, Plasma P-tau181 in Alzheimer's disease: relationship to other biomarkers,
668 differential diagnosis, neuropathology and longitudinal progression to Alzheimer's
669 dementia. *Nat Med* **26**, 379-386 (2020).
- 670 8. M. M. Mielke, C. E. Hagen, A. M. V. Wennberg, D. C. Airey, R. Savica, D. S. Knopman, M.
671 M. Machulda, R. O. Roberts, C. R. Jack, R. C. Petersen, J. L. Dage, Association of Plasma
672 Total Tau Level With Cognitive Decline and Risk of Mild Cognitive Impairment or Dementia
673 in the Mayo Clinic Study on Aging. *JAMA Neurol* **74**, 1073-1080 (2017).
- 674 9. S. Palmqvist, P. Tideman, N. Mattsson-Carlgrén, S. E. Schindler, R. Smith, R. Ossenkoppele,
675 S. Calling, T. West, M. Monane, P. B. Verghese, J. B. Braunstein, K. Blennow, S. Janelidze,
676 E. Stomrud, G. Salvado, O. Hansson, Blood Biomarkers to Detect Alzheimer Disease in
677 Primary Care and Secondary Care. *JAMA*, (2024).
- 678 10. A. A. Asuni, A. Boutajangout, D. Quartermain, E. M. Sigurdsson, Immunotherapy targeting
679 pathological tau conformers in a tangle mouse model reduces brain pathology with
680 associated functional improvements. *J Neurosci* **27**, 9115-9129 (2007).
- 681 11. A. Boutajangout, J. Ingadottir, P. Davies, E. M. Sigurdsson, Passive immunization targeting
682 pathological phospho-tau protein in a mouse model reduces functional decline and clears
683 tau aggregates from the brain. *J Neurochem* **118**, 658-667 (2011).

- 684 12. E. E. Congdon, E. M. Sigurdsson, Tau-targeting therapies for Alzheimer disease. *Nat Rev*
685 *Neurol* **14**, 399-415 (2018).
- 686 13. T. L. Rothstein, Natural Antibodies as Rheostats for Susceptibility to Chronic Diseases in
687 the Aged. *Front Immunol* **7**, 127 (2016).
- 688 14. H. U. Lutz, C. J. Binder, S. Kaveri, Naturally occurring auto-antibodies in homeostasis and
689 disease. *Trends Immunol* **30**, 43-51 (2009).
- 690 15. J. R. Jaycox, Y. Dai, A. M. Ring, Decoding the autoantibody reactome. *Science* **383**, 705-
691 707 (2024).
- 692 16. N. R. Florance, R. L. Davis, C. Lam, C. Szperka, L. Zhou, S. Ahmad, C. J. Campen, H. Moss,
693 N. Peter, A. J. Gleichman, C. A. Glaser, D. R. Lynch, M. R. Rosenfeld, J. Dalmau, Anti-N-
694 methyl-D-aspartate receptor (NMDAR) encephalitis in children and adolescents. *Ann*
695 *Neurol* **66**, 11-18 (2009).
- 696 17. V. A. Lennon, D. M. Wingerchuk, T. J. Kryzer, S. J. Pittock, C. F. Lucchinetti, K. Fujihara, I.
697 Nakashima, B. G. Weinshenker, A serum autoantibody marker of neuromyelitis optica:
698 distinction from multiple sclerosis. *Lancet* **364**, 2106-2112 (2004).
- 699 18. J. Ferrero, L. Williams, H. Stella, K. Leitermann, A. Mikulskis, J. O'Gorman, J. Sevigny, First-
700 in-human, double-blind, placebo-controlled, single-dose escalation study of aducanumab
701 (BIIB037) in mild-to-moderate Alzheimer's disease. *Alzheimers Dement (N Y)* **2**, 169-176
702 (2016).
- 703 19. A. Bartos, L. Fialová, J. Švarcová, Lower Serum Antibodies Against Tau Protein and Heavy
704 Neurofilament in Alzheimer's Disease. *J Alzheimers Dis* **64**, 751-760 (2018).
- 705 20. Y. Kronimus, A. Albus, M. Balzer-Geldsetzer, S. Straub, E. Semler, M. Otto, J. Klotsche, R.
706 Dodel, L. Consortium, D. Mengel, Naturally Occurring Autoantibodies against Tau Protein
707 Are Reduced in Parkinson's Disease Dementia. *PLoS One* **11**, e0164953 (2016).
- 708 21. M. Emmenegger, E. De Cecco, D. Lamparter, R. P. B. Jacquat, J. Riou, D. Menges, T. Ballouz,
709 D. Ebner, M. M. Schneider, I. C. Morales, B. Dogancay, J. Guo, A. Wiedmer, J. Domange,
710 M. Imeri, R. Moos, C. Zografou, L. Batkitar, L. Madrigal, D. Schneider, C. Trevisan, A.
711 Gonzalez-Guerra, A. Carrella, I. L. Dubach, C. K. Xu, G. Meisl, V. Kosmoliaptsis, T.
712 Malinauskas, N. Burgess-Brown, R. Owens, S. Hatch, J. Mongkolsapaya, G. R. Sreaton, K.
713 Schubert, J. D. Huck, F. Liu, F. Pojer, K. Lau, D. Hacker, E. Probst-Muller, C. Cervia, J.
714 Nilsson, O. Boyman, L. Saleh, K. Spanaus, A. von Eckardstein, D. J. Schaer, N. Ban, C. J. Tsai,
715 J. Marino, G. F. X. Schertler, N. Ebert, V. Thiel, J. Gottschalk, B. M. Frey, R. R. Reimann, S.
716 Hornemann, A. M. Ring, T. P. J. Knowles, M. A. Puhon, C. L. Althaus, I. Xenarios, D. I. Stuart,
717 A. Aguzzi, Continuous population-level monitoring of SARS-CoV-2 seroprevalence in a
718 large European metropolitan region. *iScience* **26**, 105928 (2023).
- 719 22. A. Senatore, K. Frontzek, M. Emmenegger, A. Chincisan, M. Losa, R. Reimann, G. Horny, J.
720 Guo, S. Fels, S. Sorce, C. Zhu, N. George, S. Ewert, T. Pietzonka, S. Hornemann, A. Aguzzi,
721 Protective anti-prion antibodies in human immunoglobulin repertoires. *EMBO Mol Med*
722 **12**, e12739 (2020).
- 723 23. M. Emmenegger, C. Zografou, D. Yile, L. R. Hoyt, R. Gudneppanavar, A. Chincisan, H.
724 Rehrauer, F. J. Noé, N. Zajac, G. Meisl, M. M. Schneider, H. Nguyen, K. Höpker, T. P. J.
725 Knowles, M. Sospedra, R. Martin, A. M. Ring, S. Leeds, S. C. Eisenbarth, M. E. Egan, E. M.
726 Bruscia, A. Aguzzi, The Cystic Fibrosis Transmembrane Regulator Controls Tolerogenic
727 Responses to Food Allergens in Mice and Humans. *medRxiv*, (2024).

- 728 24. F. A. Diaz-Quijano, A simple method for estimating relative risk using logistic regression.
729 *BMC Med Res Methodol* **12**, 14 (2012).
- 730 25. M. W. Donoghoe, I. C. Marschner, Logbin: An R Package for Relative Risk Regression Using
731 the Log-Binomial Model. *Journal of Statistical Software* **86**, (2018).
- 732 26. R. de Silva, T. Lashley, G. Gibb, D. Hanger, A. Hope, A. Reid, R. Bandopadhyay, M. Utton,
733 C. Strand, T. Jowett, N. Khan, B. Anderton, N. Wood, J. Holton, T. Revesz, A. Lees,
734 Pathological inclusion bodies in tauopathies contain distinct complements of tau with
735 three or four microtubule-binding repeat domains as demonstrated by new specific
736 monoclonal antibodies. *Neuropathol Appl Neurobiol* **29**, 288-302 (2003).
- 737 27. M. Emmenegger, E. De Cecco, M. Hruska-Plochan, T. Eninger, M. M. Schneider, M. Barth,
738 E. Tantardini, P. de Rossi, M. Bacioglu, R. G. Langston, A. Kaganovich, N. Bengoa-
739 Vergniory, A. Gonzalez-Guerra, M. Avar, D. Heinzer, R. Reimann, L. M. Hasler, T. W.
740 Herling, N. S. Matharu, N. Landeck, K. Luk, R. Melki, P. J. Kahle, S. Hornemann, T. P. J.
741 Knowles, M. R. Cookson, M. Polymenidou, M. Jucker, A. Aguzzi, LAG3 is not expressed in
742 human and murine neurons and does not modulate alpha-synucleinopathies. *EMBO Mol*
743 *Med* **13**, e14745 (2021).
- 744 28. A. Apetri, R. Crespo, J. Juraszek, G. Pascual, R. Janson, X. Zhu, H. Zhang, E. Keogh, T.
745 Holland, J. Wadia, H. Verveen, B. Siregar, M. Mrosek, R. Taggenbrock, J. Ameijde, H.
746 Inganäs, M. van Winsen, M. H. Koldijk, D. Zuijdgeest, M. Borgers, K. Dockx, E. J. M. Stoop,
747 W. Yu, E. C. Brinkman-van der Linden, K. Ummenthum, K. van Kolen, M. Mercken, S.
748 Steinbacher, D. de Marco, J. J. Hoozemans, I. A. Wilson, W. Koudstaal, J. Goudsmit, A
749 common antigenic motif recognized by naturally occurring human V. *Acta Neuropathol*
750 *Commun* **6**, 43 (2018).
- 751 29. M. P. Pase, A. S. Beiser, J. J. Himali, C. L. Satizabal, H. J. Aparicio, C. DeCarli, G. Chêne, C.
752 Dufouil, S. Seshadri, Assessment of Plasma Total Tau Level as a Predictive Biomarker for
753 Dementia and Related Endophenotypes. *JAMA Neurol* **76**, 598-606 (2019).
- 754 30. E. Barini, G. Plotzky, Y. Mordashova, J. Hoppe, E. Rodriguez-Correa, S. Julier, F. LePriault,
755 I. Mairhofer, M. Mezler, S. Biesinger, M. Cik, M. W. Meinhardt, E. Ercan-Herbst, D. E.
756 Ehrnhoefer, A. Striebinger, K. Bodie, C. Klein, L. Gasparini, K. Schlegel, Tau in the brain
757 interstitial fluid is fragmented and seeding-competent. *Neurobiol Aging* **109**, 64-77
758 (2022).
- 759 31. M. W. Donoghoe, I. C. Marschner, logbin: An R Package for Relative Risk Regression Using
760 the Log-Binomial Model. *Journal of Statistical Software* **86**, 21 (2018).
- 761 32. L. Dahm, C. Ott, J. Steiner, B. Stepniak, B. Teegen, S. Saschenbrecker, C. Hammer, K.
762 Borowski, M. Begemann, S. Lemke, K. Rentzsch, C. Probst, H. Martens, J. Wienands, G.
763 Spalletta, K. Weissenborn, W. Stöcker, H. Ehrenreich, Seroprevalence of autoantibodies
764 against brain antigens in health and disease. *Ann Neurol* **76**, 82-94 (2014).
- 765 33. Z. Y. Yu, W. W. Li, H. M. Yang, N. B. Manucat-Tan, J. Wang, Y. R. Wang, B. L. Sun, Z. C. Hu,
766 L. L. Zhang, L. Tan, J. Deng, Y. H. Liu, Naturally Occurring Antibodies to Tau Exists in Human
767 Blood and Are Not Changed in Alzheimer's Disease. *Neurotox Res* **37**, 1029-1035 (2020).
- 768 34. Y. Tsuboi, R. J. Uitti, M. B. Delisle, J. J. Ferreira, C. Brefel-Courbon, O. Rascol, B. Ghetti, J.
769 R. Murrell, M. Hutton, M. Baker, Z. K. Wszolek, Clinical features and disease haplotypes
770 of individuals with the N279K tau gene mutation: a comparison of the pallidopontonigral
771 degeneration kindred and a French family. *Arch Neurol* **59**, 943-950 (2002).

- 772 35. I. Sotiropoulos, M. C. Galas, J. M. Silva, E. Skoulakis, S. Wegmann, M. B. Maina, D. Blum,
773 C. L. Sayas, E. M. Mandelkow, E. Mandelkow, M. G. Spillantini, N. Sousa, J. Avila, M.
774 Medina, A. Mudher, L. Buee, Atypical, non-standard functions of the microtubule
775 associated Tau protein. *Acta Neuropathol Commun* **5**, 91 (2017).
- 776 36. M. M. Rinschen, M. Gödel, F. Grahammer, S. Zschiedrich, M. Helmstädter, O. Kretz, M.
777 Zarei, D. A. Braun, S. Dittrich, C. Pahmeyer, P. Schroder, C. Teetzen, H. Gee, G. Daouk, M.
778 Pohl, E. Kuhn, B. Schermer, V. Küttner, M. Boerries, H. Busch, M. Schiffer, C. Bergmann,
779 M. Krüger, F. Hildebrandt, J. Dengjel, T. Benzing, T. B. Huber, A Multi-layered Quantitative
780 In Vivo Expression Atlas of the Podocyte Unravels Kidney Disease Candidate Genes. *Cell*
781 *Rep* **23**, 2495-2508 (2018).
- 782 37. K. H. Ho, X. Yang, A. B. Osipovich, O. Cabrera, M. L. Hayashi, M. A. Magnuson, G. Gu, I.
783 Kaverina, Glucose Regulates Microtubule Disassembly and the Dose of Insulin Secretion
784 via Tau Phosphorylation. *Diabetes* **69**, 1936-1947 (2020).
- 785 38. L. Vallés-Saiz, R. Peinado-Cahuchola, J. Ávila, F. Hernández, Microtubule-associated
786 protein tau in murine kidney: role in podocyte architecture. *Cell Mol Life Sci* **79**, 97 (2022).
- 787 39. E. E. Congdon, C. Ji, A. M. Tetlow, Y. Jiang, E. M. Sigurdsson, Tau-targeting therapies for
788 Alzheimer disease: current status and future directions. *Nat Rev Neurol* **19**, 715-736
789 (2023).
- 790 40. *ClinicalTrials.gov*, NCT05269394, *Dominantly Inherited Alzheimer Network Trial: An*
791 *Opportunity to Prevent Dementia. A Study of Potential Disease Modifying Treatments in*
792 *Individuals With a Type of Early Onset Alzheimer's Disease Caused by a Genetic Mutation*
793 *(DIAN-TU)*,
794 ([https://clinicaltrials.gov/study/NCT05269394?cond=Alzheimer%20Disease&term=E281](https://clinicaltrials.gov/study/NCT05269394?cond=Alzheimer%20Disease&term=E2814&rank=1)
795 [4&rank=1](https://clinicaltrials.gov/study/NCT05269394?cond=Alzheimer%20Disease&term=E2814&rank=1)) (2023).
- 796 41. M. E. Barton, B. Van Den Steen, H. L. G. Van Tricht, W. Byrnes, F. E. Purcell, S. A. Southcott,
797 D. Raby, Y. I. Starshinov, C. Ewen, Update on the TOGETHER study: a patient- and
798 investigator-blind, randomized, placebo-controlled study evaluating the efficacy, safety
799 and tolerability of bepranemab, UCB0107, in prodromal-to-mild Alzheimer's disease.
800 *Alzheimer's & Dementia* **18**, e068973 (2022).
- 801 42. A. Moscoso, M. J. Grothe, N. J. Ashton, T. K. Karikari, J. Lantero Rodríguez, A. Snellman,
802 M. Suárez-Calvet, K. Blennow, H. Zetterberg, M. Schöll, A. s. D. N. Initiative, Longitudinal
803 Associations of Blood Phosphorylated Tau181 and Neurofilament Light Chain With
804 Neurodegeneration in Alzheimer Disease. *JAMA Neurol* **78**, 396-406 (2021).
- 805 43. N. R. Barthélemy, Y. Li, N. Joseph-Mathurin, B. A. Gordon, J. Hassenstab, T. L. S. Benzinger,
806 V. Buckles, A. M. Fagan, R. J. Perrin, A. M. Goate, J. C. Morris, C. M. Karch, C. Xiong, R.
807 Allegri, P. C. Mendez, S. B. Berman, T. Ikeuchi, H. Mori, H. Shimada, M. Shoji, K. Suzuki, J.
808 Noble, M. Farlow, J. Chhatwal, N. R. Graff-Radford, S. Salloway, P. R. Schofield, C. L.
809 Masters, R. N. Martins, A. O'Connor, N. C. Fox, J. Levin, M. Jucker, A. Gabelle, S. Lehmann,
810 C. Sato, R. J. Bateman, E. McDade, D. I. A. Network, A soluble phosphorylated tau
811 signature links tau, amyloid and the evolution of stages of dominantly inherited
812 Alzheimer's disease. *Nat Med* **26**, 398-407 (2020).
- 813 44. T. K. Karikari, T. A. Pascoal, N. J. Ashton, S. Janelidze, A. L. Benedet, J. L. Rodriguez, M.
814 Chamoun, M. Savard, M. S. Kang, J. Therriault, M. Schöll, G. Massarweh, J. P. Soucy, K.
815 Höglund, G. Brinkmalm, N. Mattsson, S. Palmqvist, S. Gauthier, E. Stomrud, H. Zetterberg,

- 816 O. Hansson, P. Rosa-Neto, K. Blennow, Blood phosphorylated tau 181 as a biomarker for
817 Alzheimer's disease: a diagnostic performance and prediction modelling study using data
818 from four prospective cohorts. *Lancet Neurol* **19**, 422-433 (2020).
- 819 45. J. C. Park, S. H. Han, D. Yi, M. S. Byun, J. H. Lee, S. Jang, K. Ko, S. Y. Jeon, Y. S. Lee, Y. K. Kim,
820 D. Y. Lee, I. Mook-Jung, Plasma tau/amyloid- β 1-42 ratio predicts brain tau deposition and
821 neurodegeneration in Alzheimer's disease. *Brain* **142**, 771-786 (2019).
- 822 46. S. Palmqvist, S. Janelidze, Y. T. Quiroz, H. Zetterberg, F. Lopera, E. Stomrud, Y. Su, Y. Chen,
823 G. E. Serrano, A. Leuzy, N. Mattsson-Carlgrén, O. Strandberg, R. Smith, A. Villegas, D.
824 Sepulveda-Falla, X. Chai, N. K. Proctor, T. G. Beach, K. Blennow, J. L. Dage, E. M. Reiman,
825 O. Hansson, Discriminative Accuracy of Plasma Phospho-tau217 for Alzheimer Disease vs
826 Other Neurodegenerative Disorders. *JAMA* **324**, 772-781 (2020).
- 827 47. K. Yanamandra, T. K. Patel, H. Jiang, S. Schindler, J. D. Ulrich, A. L. Boxer, B. L. Miller, D. R.
828 Kerwin, G. Gallardo, F. Stewart, M. B. Finn, N. J. Cairns, P. B. Verghese, I. Fogelman, T.
829 West, J. Braunstein, G. Robinson, J. Keyser, J. Roh, S. S. Knapik, Y. Hu, D. M. Holtzman,
830 Anti-tau antibody administration increases plasma tau in transgenic mice and patients
831 with tauopathy. *Sci Transl Med* **9**, (2017).
- 832 48. M. M. Mielke, J. L. Dage, R. D. Frank, A. Algeciras-Schimnich, D. S. Knopman, V. J. Lowe,
833 G. Bu, P. Vemuri, J. Graff-Radford, C. R. Jack, Jr., R. C. Petersen, Performance of plasma
834 phosphorylated tau 181 and 217 in the community. *Nat Med* **28**, 1398-1405 (2022).
- 835 49. C. M. Hedgepeth, L. J. Conrad, J. Zhang, H. C. Huang, V. M. Lee, P. S. Klein, Activation of
836 the Wnt signaling pathway: a molecular mechanism for lithium action. *Dev Biol* **185**, 82-
837 91 (1997).
- 838 50. J. J. Bunker, S. A. Erickson, T. M. Flynn, C. Henry, J. C. Koval, M. Meisel, B. Jabri, D. A.
839 Antonopoulos, P. C. Wilson, A. Bendelac, Natural polyreactive IgA antibodies coat the
840 intestinal microbiota. *Science* **358**, (2017).
- 841 51. H. Mouquet, J. F. Scheid, M. J. Zoller, M. Krogsgaard, R. G. Ott, S. Shukair, M. N. Artyomov,
842 J. Pietzsch, M. Connors, F. Pereyra, B. D. Walker, D. D. Ho, P. C. Wilson, M. S. Seaman, H.
843 N. Eisen, A. K. Chakraborty, T. J. Hope, J. V. Ravetch, H. Wardemann, M. C. Nussenzweig,
844 Polyreactivity increases the apparent affinity of anti-HIV antibodies by heteroligation.
845 *Nature* **467**, 591-595 (2010).
- 846 52. B. R. Hoover, M. N. Reed, J. Su, R. D. Penrod, L. A. Kotilinek, M. K. Grant, R. Pitstick, G. A.
847 Carlson, L. M. Lanier, L. L. Yuan, K. H. Ashe, D. Liao, Tau mislocalization to dendritic spines
848 mediates synaptic dysfunction independently of neurodegeneration. *Neuron* **68**, 1067-
849 1081 (2010).
- 850 53. L. A. McNutt, C. Wu, X. Xue, J. P. Hafner, Estimating the relative risk in cohort studies and
851 clinical trials of common outcomes. *Am J Epidemiol* **157**, 940-943 (2003).
- 852 54. M. Emmenegger, V. Emmenegger, S. M. Shambat, T. C. Scheier, A. Gomez-Mejia, C. C.
853 Chang, P. D. Wendel-Garcia, P. K. Buehler, T. Buettner, D. Roggenbuck, S. D. Brugger, K.
854 B. M. Frauenknecht, Antiphospholipid antibodies are enriched post-acute COVID-19 but
855 do not modulate the thrombotic risk. *Clin Immunol* **257**, 109845 (2023).
- 856 55. M. Emmenegger, V. Emmenegger, in *Zenodo*, <https://doi.org/10.5281/zenodo.10051979>.
857 (2023).
- 858 56. M. Losa, M. Emmenegger, P. De Rossi, P. M. Schürch, T. Serdiuk, N. Pengo, D. Capron, D.
859 Bieli, N. J. Rupp, M. C. Carta, K. J. Karl J Frontzek, V. Lysenko, R. R. Reimann, A. K. K.

- 860 Lakkaraju, M. Nuvolone, G. T. Westermark, K. P. R. Nilsson, M. Polymenidou, A. P. A.
861 Theocharides, Simone Hornemann, P. Picotti, A. Aguzzi, The ASC inflammasome adapter
862 controls the extent of peripheral protein aggregate deposition in inflammation-
863 associated amyloidosis. *BioRxiv*, doi: <https://doi.org/10.1101/2021.05.01.442282>, (2023).
864 57. C. D. Orrú, J. Yuan, B. S. Appleby, B. Li, Y. Li, D. Winner, Z. Wang, Y. A. Zhan, M. Rodgers,
865 J. Rarick, R. E. Wyza, T. Joshi, G. X. Wang, M. L. Cohen, S. Zhang, B. R. Groveman, R. B.
866 Petersen, J. W. Ironside, M. E. Quiñones-Mateu, J. G. Safar, Q. Kong, B. Caughey, W. Q.
867 Zou, Prion seeding activity and infectivity in skin samples from patients with sporadic
868 Creutzfeldt-Jakob disease. *Sci Transl Med* **9**, (2017).
869 58. RStudioTeam. (RStudio, PBC, Boston, MA, 2021).

870

871 **Acknowledgments:**

872 The authors wish to thank the hospital patients and blood donors for their generous altruistic con-
873 tributions to this study. Imaging was performed with equipment maintained by the Center for Mi-
874 croscopy and Image Analysis, University of Zurich. We thank Prof. Rohan de Silva (UCL Queen
875 Square Institute of Neurology, London, UK) for providing the purified anti-MTBD-tau antibody
876 RD4. We thank Dr. Marco Losa for the generous provision of secondary antibodies for light chain
877 typing and Magdalena Bialkowska, Lisa Cafilisch, Berre Doğançay, Julie Domange, Marigona
878 Imeri, Lorène Mottier, Rea Müller, Antonella Rosati, Dezirae Schneider, and Anne Wiedmer for
879 help with the high-throughput assays. Insightful advice about programming in R software was
880 provided by Reto Guadagnini.

881

882 **Funding:**

883 University of Zürich, Candoc grant FK-19-025 (ADM)
884 Swiss Personalised Health Network, SPHN, driver project grant 2017DRI17 (AA)
885 Swiss National Foundation SNF (SNSF grant ID 179040 and grant ID 207872, Sinergia grant ID
886 183563) (AA)
887 European Research Council ERC Prion2020, 670958 (AA)
888 Nomis Foundation (AA)
889 Innovation Fund of the University Hospital Zurich (INOV00096) (AA)
890 University Hospital Zurich Foundation grant USZF27101 (with contributions of the NOMIS Foun-
891 dation, the Schwyzer Winiker Stiftung, and the Baugarten Stiftung, AA, ME)
892 HMZ ImmunoTarget grant, Stiftung Neuropath and GELU Foundation (AA)

893 Michael J. Fox Foundation (grant ID MJFF-020710 and MJFF-021073) (SH).

894

895 **Author contributions:**

896 Conceived and designed the experiments: ADM, SH, AA. Supervised the study: SH, AA. Per-
897 formed tau protein purification: ADM, EDC, JG. Performed tau microELISA automated screen:
898 ADM, ME. Performed amyloid- β pyroglutamate and cellular prion protein microELISA auto-
899 mated screen: MC, KF, ME. Maintained microELISA automated platform: ME. Performed puri-
900 fication, validation and characterization of anti-tau autoantibodies: ADM, JG. Maintained the clin-
901 ical database: ME, AC. Performed data analysis and visualization: ADM. Wrote the first draft of
902 manuscript: ADM. Corrected and advised on subsequent versions of the manuscript: ADM, ME,
903 SH, AA. All authors reviewed and approved the final version of the manuscript and consented to
904 be accountable for the work.

905

906 **Competing interests:**

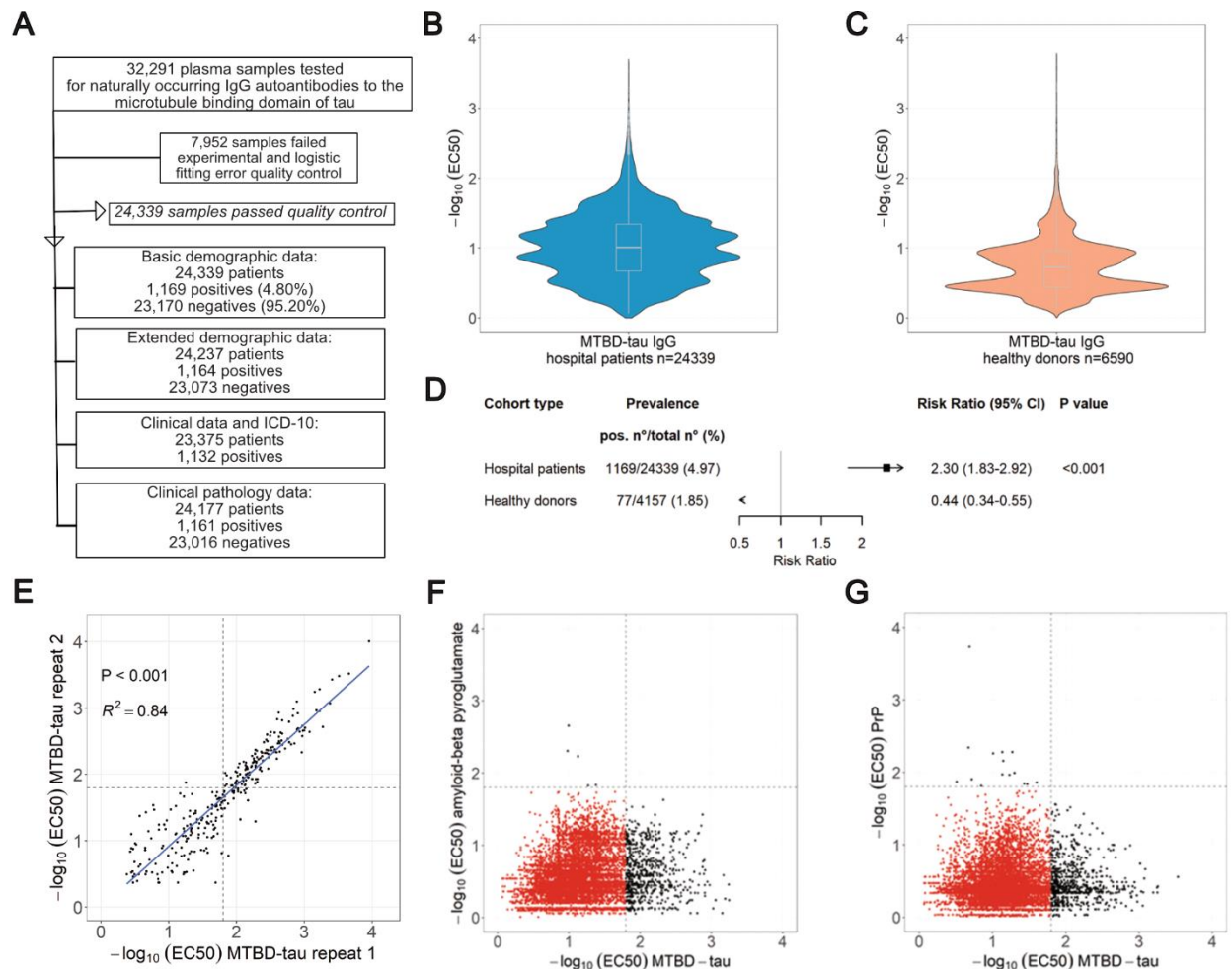
907 ADM has received a research grant from University of Zurich; KF has received research grants
908 from Ono Pharmaceuticals and Theodor Ida Herzog Egli Stiftung, consulting fees from Acumen
909 Collective and Ionis Pharmaceuticals, support for attending meetings/travel from Euro-CNS and
910 has participated on the Advisory Board of Mabyron AG; AA has received research grants from the
911 Swiss Personalized Health Network, Swiss National Foundation, European Research Council and
912 Nomis Foundation and is a member of the Board of Directors of Mabyron AG. Mabyron AG pro-
913 duces therapeutic human antibodies. Mabyron AG had no insight and no influence on the current
914 study. All authors report no other relationships or activities that could appear to have influenced
915 the submitted work.

916

917 **Data and materials availability:**

918 Data and material requests should be addressed to the corresponding authors. Materials will be
919 shared upon reasonable request, given the approval by an ethics committee or review board and a
920 material transfer agreement.

921 **Figures**



Magalhães et al, Figure 1

922

923

924 **Fig. 1. Study overview and seroprevalence of anti-MTBD-tau IgG autoantibodies. A.**

925 Flowchart of the study design. **B.-C.** Distribution of $-\log_{10}(\text{EC}_{50})$ values obtained from the micro-

926 ELISA screen of hospital (B) and blood donor (C) plasma samples. **D.** Age- and sex-adjusted risk

927 ratio ratios and 95% confidence intervals (CI; I bars) for the detection of anti-tau autoantibodies

928 in hospital and blood-bank plasma samples. **E.** Replicability of microELISA duplicates with inde-

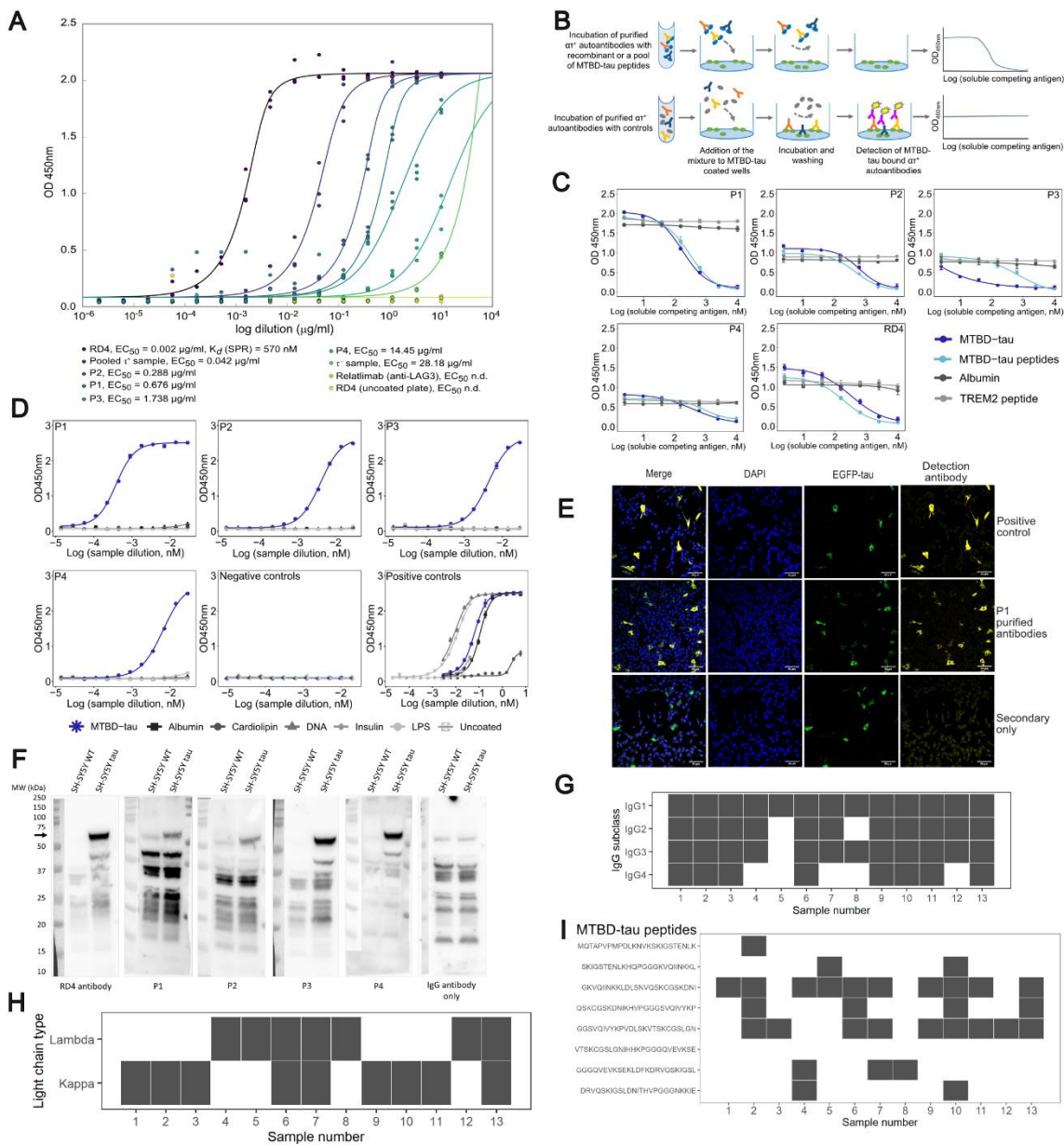
929 pendent estimation of the $-\log_{10}(\text{EC}_{50})$ values. Dashed lines: cut-off value of $-\log_{10}(\text{EC}_{50}) = 1.8$. **F.**

930 $-\log_{10}(\text{EC}_{50})$ values of samples tested by microELISA against MTBD-tau and amyloid- β pyroglu-

931 tamate. **G.** Same as shown in (F), but for samples tested against MTBD-tau and the cellular prion

932 protein (PrP^C).

933

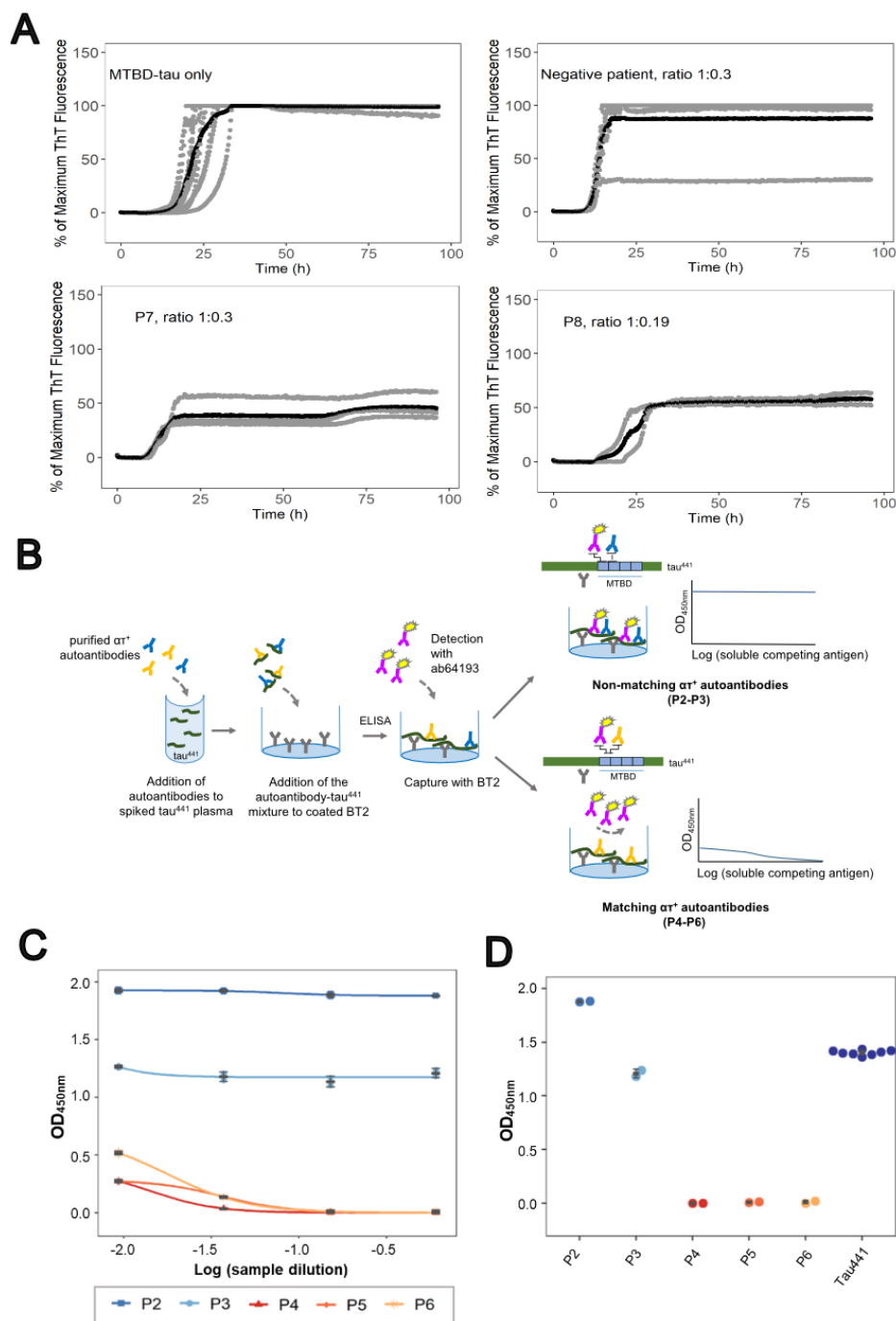


934

Magalhães et al, Figure 2

935 **Fig. 2. Biophysical characterization of samples from α^+ patients.** A. Indirect ELISA of purified anti-MTBD-tau autoantibodies from four α^+ samples and from 6 pooled α^+ samples. All antibodies were assayed at the same concentration to compare their EC_{50} to that of RD4. EC_{50} values are indicated in the Figure. n.d.: not determined. B. Principle of competition ELISA. C. Competition ELISA of purified anti-tau autoantibodies from four α^+ patients against albumin, 939 recombinant MTBD-tau, synthetic peptides spanning the sequence of MTBD-tau and synthetic 940 TREM2 RD4 (anti-4-repeat-isoform) antibody: positive control. Mean values \pm SD of two repli- 941

942 cates. **D.** Indirect ELISA to assess the reactivity of purified anti-tau autoantibodies against albu-
943 min, cardiolipin, double-stranded DNA, insulin, lipopolysaccharides (LPS), MTBD-tau and un-
944 coated plates. Positive controls were as follows: RD4 antibody for MTBD-tau, anti-DNP antibody
945 for cardiolipin, albumin and DNA and the IKC pool of 20 heparin plasma samples for insulin, LPS
946 and uncoated plates. Mean values \pm SD of two replicates are shown. **E.** Representative immuno-
947 fluorescence images of SH-SY5Y cells expressing EGFP-0N4R-tau using affinity-purified anti-
948 tau autoantibodies. HT7 pan-tau antibody: positive control. No primary antibody: negative control.
949 Scale bar: 60 μ m. **F.** Western blot of cell lysates from wild-type (SH-SY5Y WT) or tau^{P301L/S320F}-
950 overexpressing cells (SH-SY5Y tau) using purified anti-tau autoantibodies from four $\alpha\tau^+$ patients.
951 Positive control: RD4. Negative control: omission of primary antibody. **G.** IgG subclass typing of
952 13 $\alpha\tau^+$ plasma samples. Gray and white boxes: reactive and non-reactive samples, respectively. **H.**
953 κ/λ light chain typing of the samples in F. **I.** Epitope mapping of the samples in Fig. 2F against
954 25mer MTBD-tau peptides with 10 residues overlap. Vertical axis: sequences of the MTBD-tau
955 peptides covering the sequence of MTBD-tau.

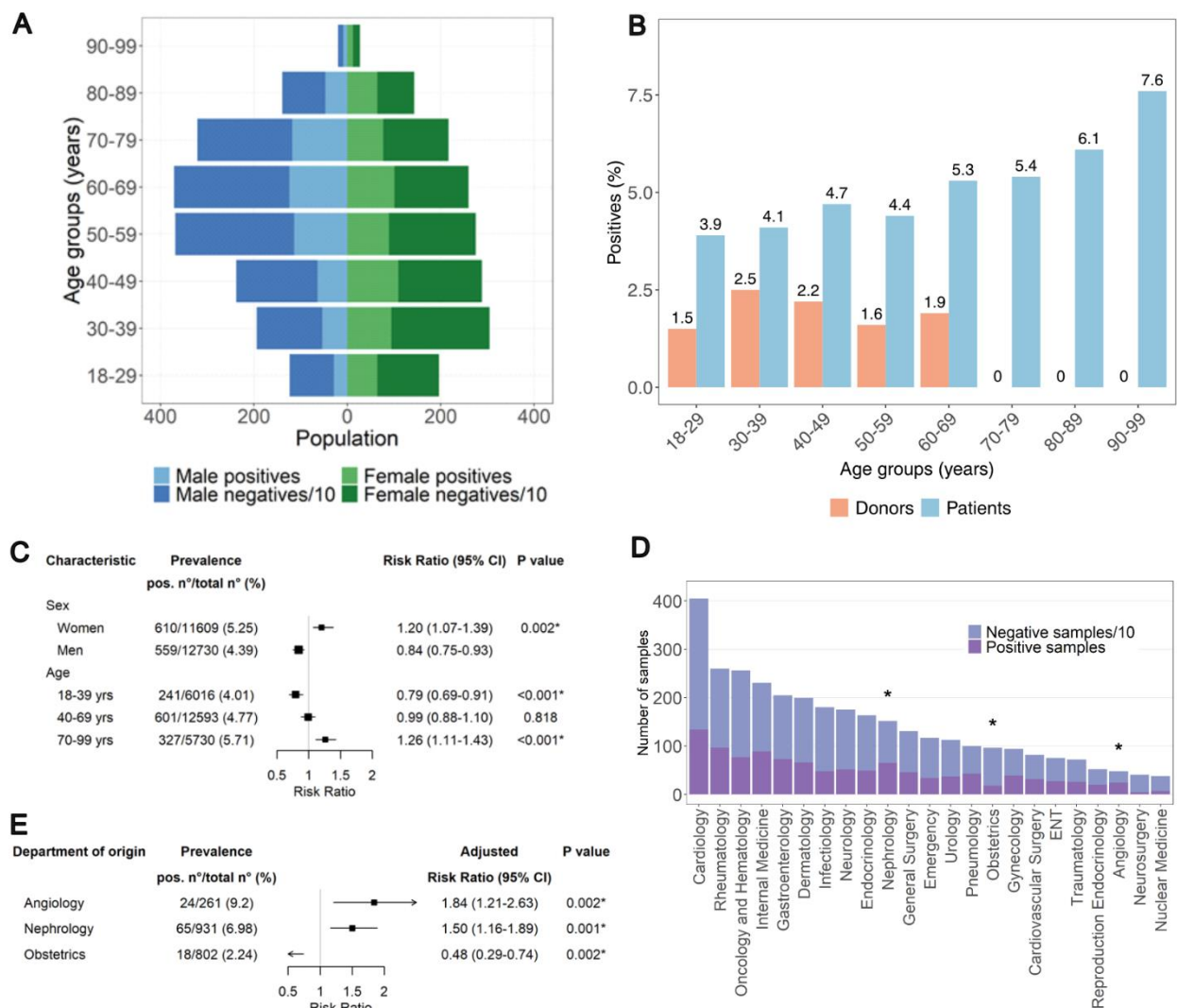


Magalhães et al, Figure 3

956
 957 **Fig. 3. Natural $\alpha\tau$ autoantibodies inhibit tau aggregation and impair tau detection. A.** Kinetic
 958 aggregation curves of MTBD-tau followed by ThT fluorescence in the absence ($n=12$) or presence
 959 of purified $\alpha\tau$ autoantibodies (patient P7 ($n=4$) and P8 ($n=2$)) or antibodies from an $\alpha\tau^-$ sample
 960 ($n=6$). Stoichiometric ratios as indicated. Gray lines indicate individual replicates and black lines
 961 the average of the replicates. **B.** Principle of the competition sandwich ELISA. **C.** Competitive

962 sandwich ELISA to assess the ability of purified anti-tau autoantibodies with matching (P4-P6)
963 and non-matching (P2 and P3) epitopes to the commercial detection antibody, ab64193, to impair
964 the detection of free tau⁴⁴¹ spiked in plasma (dark blue). Serial dilutions of purified anti-tau anti-
965 bodies are shown in (C) and binding at highest anti-tau antibody concentrations in (D).
966

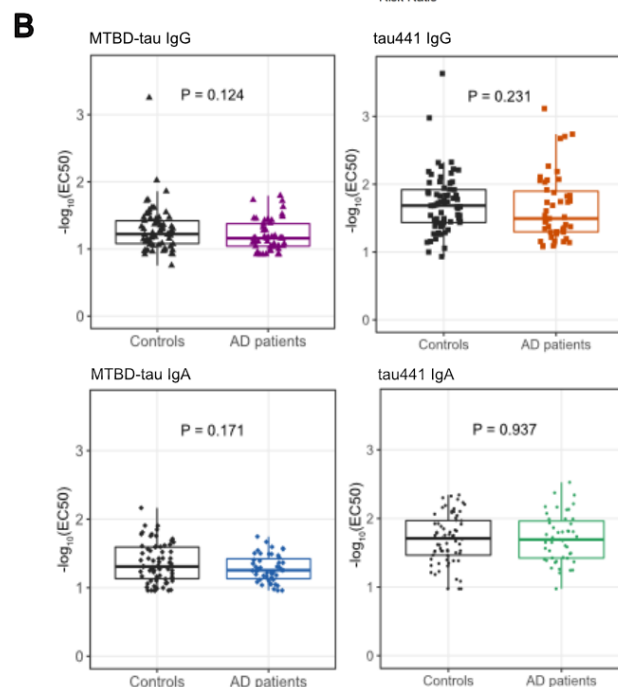
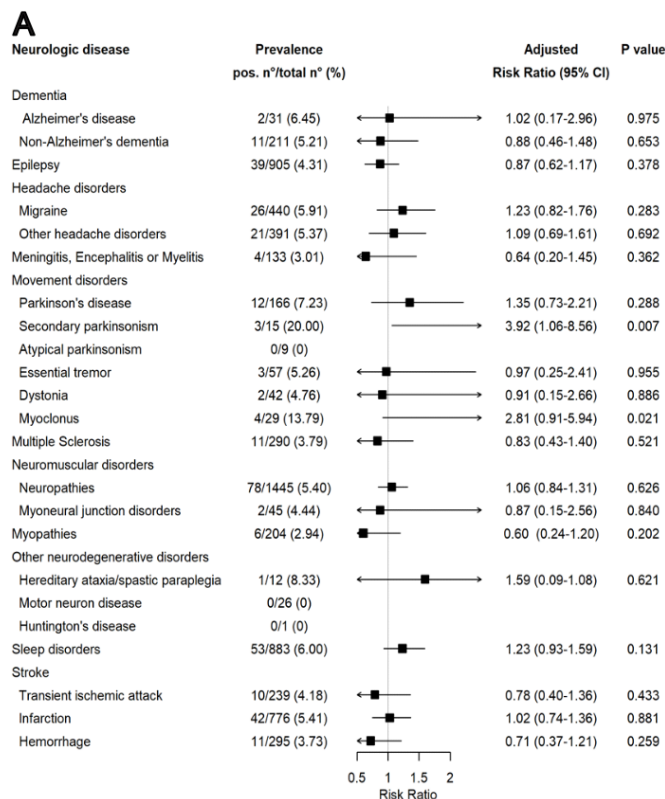
967



Magalhães et al, Figure 4

968

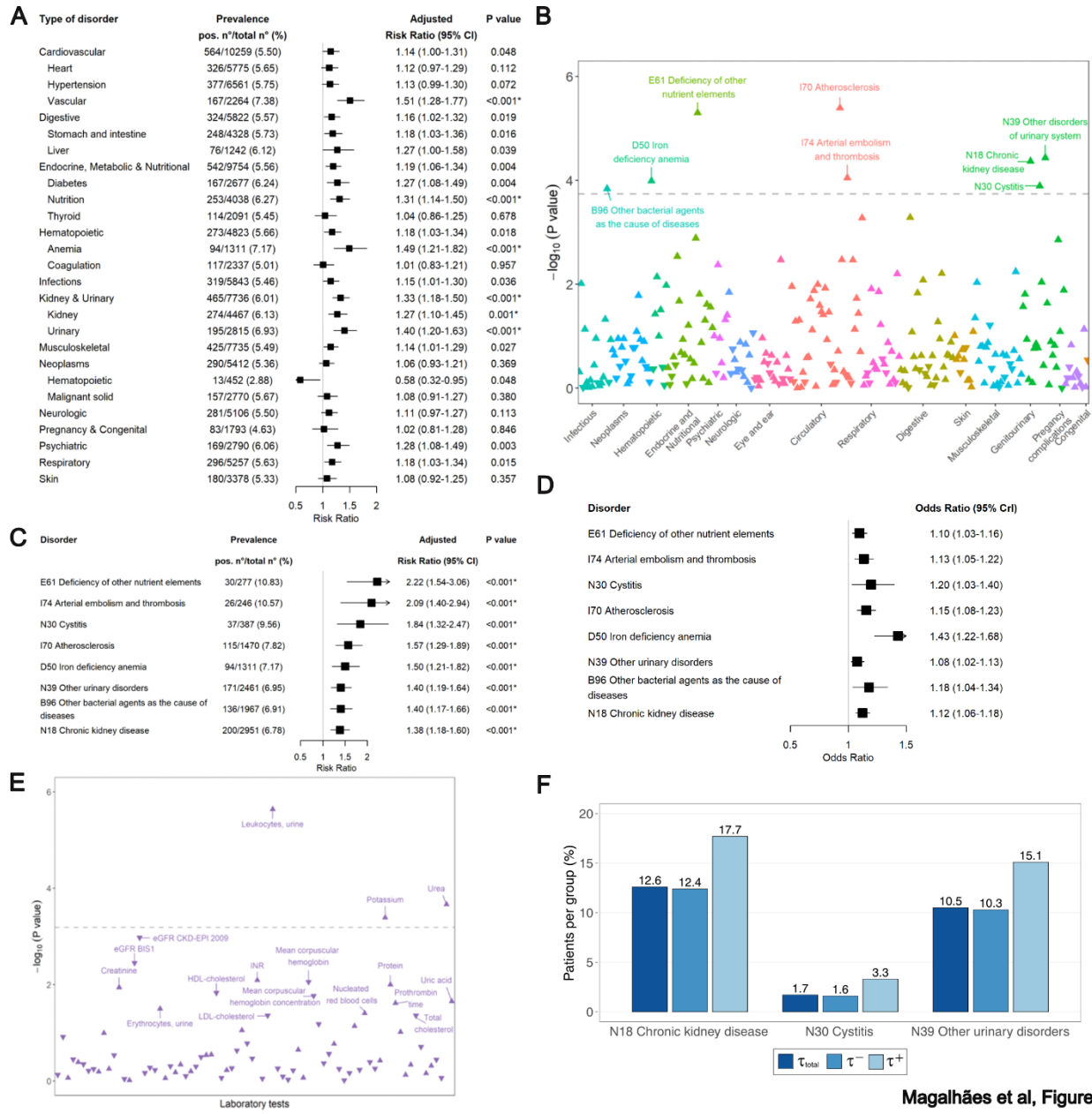
969 **Fig. 4. Demographic characteristics of hospital patients' cohort.** **A.** Age and sex pyramid of
 970 positive and negative individuals. **B.** Percentage of positives across decadic age groups. The num-
 971 bers on top of each bar correspond to the positivity rates. Numbers inside bars: α^+ vs tested sam-
 972 ples in each age group. χ^2 test for trend in proportions. **C.** Risk ratios \pm 95% confidence intervals
 973 (CI) for α^+ autoantibodies according to sex and age groups. Asterisks: $P < 0.05$ after Bonferroni
 974 correction. **D.** Break-down of samples by clinical department. Asterisks: $P < 0.05$ (two-proportions
 975 z-test with Bonferroni correction). **E.** Age- and sex-adjusted risk ratios \pm 95% CI for α^+ samples
 976 by clinical department. Asterisks: $P < 0.05$ after Bonferroni correction.



Magalhães et al, Figure 5

977
 978 **Fig. 5. Age- and sex-adjusted risk ratios of MTBD-tau-autoreactivity for major groups of**
 979 **neurological disorders and reactivity profiles for AD screen. A. Age- and sex-adjusted risk**
 980 **ratios and 95% confidence intervals (CI; I bars) for $\alpha\tau^+$ autoantibodies according to different**

981 groups of neurological disorders. No P values remained significant after Bonferroni correction. **B.**
982 Boxplots showing the 25th, 50th (median) and 75th percentiles of the reactivity profiles for AD and
983 control patients (Mann-Whitney U test).
984



985

986 **Fig. 6. Association of MTBD-tau IgG autoantibodies and systemic disorders and clinical laboratory data.** **A.** Age- and sex-adjusted risk ratios \pm 95% CI (bars) for $\alpha\tau^+$ autoantibodies
 987 **grouped 27 different main systemic clinical conditions.** Asterisks: $P < 0.05$ after Bonferroni cor-
 988 **rection.** **B.** $-\log_{10}(P \text{ value})$ of the log-binomial regression for the presence of plasma MTBD-tau
 989 **IgG autoantibodies for 276 disorders according to ICD-10 codes and adjusted for age and sex.**
 990 **Triangles pointing upwards and downwards: positive and coefficients, respectively; gray dashed**
 991 **line: $P < 0.05$ after Bonferroni correction (here and henceforth). P values significant after Bonfer-**
 992

993 roni adjustment are labelled with the ICD codes. **C.** Same as (A), but according to individual dis-
994 ease entities from (B). **D.** Bayesian logistic regression adjusted for age and sex on ICD-10 codes
995 significantly associated in B. and using $-\log_{10}(\text{EC}_{50})$ as continuous outcome (odds ratio \pm 95%
996 credible intervals). This analysis confirms the positive association of these ICD-10 codes with $\alpha\tau$
997 reactivity (from B). **E.** $-\log_{10}(\text{P value})$ of the log-binomial regression for the presence of plasma
998 MTBD-tau IgG autoantibodies and clinical laboratory parameters. P values significant after Bon-
999 ferroni adjustment are labelled with the ICD codes. The gray dashed line indicates the significance
1000 level after Bonferroni correction ($<0.05/106=0.00047$). eGFR CKD-EPI 2009: estimated glomer-
1001 ular filtration rate using the Chronic Kidney Disease Epidemiology Collaboration 2009 equation;
1002 eGFR BIS1: estimated glomerular filtration rate using the older adults Berlin Initiative Study 1
1003 equation. INR: international normalized ratio. LDL: low-density lipoprotein. HDL: high-density
1004 lipoprotein. **F.** Calculated prevalence of different ICD-10 codes in the total cohort (dark blue), $\alpha\tau^-$
1005 ($\alpha\tau^+$ samples (light blue).